

## Coupled ocean–atmosphere modeling and predictions

by Arthur J. Miller<sup>1,2</sup>, Mat Collins<sup>3</sup>, Silvio Gualdi<sup>4</sup>, Tommy G. Jensen<sup>5</sup>,  
Vasu Misra<sup>6</sup>, Luciano Ponzi Pezzi<sup>7</sup>, David W. Pierce<sup>1</sup>, Dian Putrasahan<sup>8</sup>,  
Hyodae Seo<sup>9</sup>, and Yu-Heng Tseng<sup>10</sup>

### ABSTRACT

Key aspects of the current state of the ability of global and regional climate models to represent dynamical processes and precipitation variations are summarized. Interannual, decadal, and global-warming timescales, wherein the influence of the oceans is relevant and the potential for predictability is highest, are emphasized. Oceanic influences on climate occur throughout the ocean and extend over land to affect many types of climate variations, including monsoons, the El Niño Southern Oscillation, decadal oscillations, and the response to greenhouse gas emissions. The fundamental ideas of coupling between the ocean-atmosphere-land system are explained for these modes in both global and regional contexts. Global coupled climate models are needed to represent and understand the complicated processes involved and allow us to make predictions over land and sea. Regional coupled climate models are needed to enhance our interpretation of the fine-scale response. The mechanisms by which large-scale, low-frequency variations can influence shorter timescale variations and drive regional-scale effects are also discussed. In this light of these processes, the prospects for practical climate predictability are also presented.

*Keywords:* climate modeling, regional climate downscaling, climate predictability, El Niño Southern Oscillation, ENSO, global warming, monsoons, decadal climate variability, ocean-atmosphere-land interactions

### 1. Introduction

The ocean exerts a strong influence on the atmospheric circulation and precipitation, both due to the oceanic mean state and its anomalies. These influences occur throughout

1. Scripps Institution of Oceanography, La Jolla, CA USA 92093
2. Corresponding author: *e-mail: ajmiller@ucsd.edu*
3. University of Exeter, Exeter, UK EX4 4QF
4. Centro Euro-Mediterraneo sui Cambiamenti Climatici, Bologna, Italy 40127
5. Naval Research Laboratory, Stennis Space Center, MS USA 39529
6. Florida State University, Tallahassee, FL USA 32306
7. National Institute for Space Research, São José dos Campos SP, Brazil 12227
8. Max Planck Institute for Meteorology, Hamburg, Germany 20146
9. Woods Hole Oceanographic Institution, Woods Hole, MA USA 02543
10. National Taiwan University, Taipei, Taiwan 10673

the ocean, extend over land, and affect many timescales of variability, including monsoons, the El Niño Southern Oscillation (ENSO), decadal modes, and the response to greenhouse gas emissions. Global coupled climate models are needed to represent and understand the complicated processes involved and allow us to make predictions over land and sea. Regional coupled climate models are needed to enhance our interpretation of the fine-scale response.

This paper focuses on the fundamental coupling within the ocean–atmosphere–land system, particularly as it affects precipitation, in both global and regional contexts. We focus here on interannual to decadal variations of the large-scale system. We also discuss how those large-scale, low-frequency variations can influence shorter timescale variations and how the system can be downscaled to understand local impacts.

Our goal is to summarize key aspects of the current state of global and regional climate models, focusing on their ability to represent dynamical and precipitation processes on interannual, decadal, and global-warming timescales, for which the influence of the oceans is relevant and the potential for predictability is emphasized.

## **2. Global climate models**

A primary goal of global climate modeling and prediction is to properly represent the wide range of processes that occur in the air–sea–ice–land system (Palmer 2014). Current climate model capabilities include fully coupled atmosphere, ocean, wave, sea ice, and land surface models with typically about 100-km resolution (e.g., Taylor et al. 2012). They are readily capable of simulating many aspects of observed climate variability, as will be highlighted in subsequent sections. These models are also often extended to include biogeochemical cycles and ecosystem models, but this will not be the focus of this discussion.

The accuracy of numerical simulations relies on the ability of atmospheric and oceanic models to capture the essential physics of the phenomena involved. Models used for climate studies and seasonal forecasting attempt to represent all the important physical processes that affect ocean–atmosphere–land interactions. Modeling the freshwater evaporation–precipitation feedback loop, transport of moisture in the atmosphere, and regional rainfall is a major focus for global coupled models (IPCC 2013). Cloud formation and condensation processes, however, are highly nonlinear and sensitive to model formulation. Model rainfall over land must fall within the proper drainage basin, and once river runoff reaches the shore, stirring by tidal, mesoscale, and submesoscale currents must generate salinity fronts where stirring and flow instabilities can take place and produce mixing into the water column. This downward mixing often takes place during nighttime cooling, which thereby requires resolving the diurnal cycle; this is commonly missing in the climate models. Rainfall over the sea results in low-salinity water lenses that can affect the vertical stability of the ocean boundary layer. Under calm, clear sky conditions, sea surface temperature (SST) will rapidly increase, which in turn can lead to convective clouds and more precipitation, i.e., a positive feedback.

A major challenge to properly resolve the air–sea–ice–land coupling in climate models is the coupling framework. There are several standard couplers available to the community, for example the OASIS (ENES 2011), the Model Coupling Toolkit (MCT; USDOE 2015), and the Earth System Modeling Framework (ESMF; ESGF-CoG 2017). But many models are also based on a coupler developed by their own coupling algorithms in order to improve the efficiency and performance (e.g., GFDL Flexible Modeling System). Coupling is done either concurrently or sequentially, with the coupling frequency ranging from hourly to daily, although some models couple at every model time-step for operational purposes. Couplers differ in how they calculate the surface fluxes: some use the surface fluxes obtained directly from the nonlocal surface physics scheme of the atmosphere, while others use the simple bulk formula in the coupler, given the lower meteorological variables provided by the atmosphere and the ocean surface properties.

Climate model biases are well known to occur in global climate models (GCMs) and major international research efforts continually attempt to remedy them. The biases degrade climate simulations of natural and forced variability and deteriorate climate forecasts of future conditions (Turner et al. 2007b; Gent et al. 2010; Kay et al. 2012; National Research Council 2012). Of particular concern are the biases that develop in the tropical Pacific Ocean because of it being the source of ENSO variability, which extends its influence through teleconnections around the globe (Pezzi and Cavalcanti 2001; Turner et al. 2007a; Deser et al. 2011; Lienert et al. 2011; Xiang et al. 2011; Wang et al. 2017). Fully coupled models tend to have a cold bias in the cold tongue region when simulating the eastern equatorial Pacific, which may be partially caused by the poor representation of Tropical Instability Waves (TIW) activity (Pezzi 2003; Pezzi and Richards 2003; Pezzi et al. 2004). Also, the majority of coupled models show the occurrence of an overly strong Intertropical Convergence Zone (ITCZ) in the southeastern Pacific region (Mechoso et al. 1995; Bellucci et al. 2010). Though the appearance of a Southern Hemispheric ITCZ is observed during March–April in the tropical Pacific, its overestimation represents a well-known bias affecting state-of-the-art climate models, which is generally referred to as double ITCZ (Mechoso et al. 1995).

The tropical Pacific biases also impact the propagation of Madden-Julian Oscillation (MJO) disturbances as they transit the Pacific and affect distant regions such as western North America (Jones 2000; Hendon et al. 2007; Sardeshmukh and Sura 2007; Tang and Yu 2008; Marshall et al. 2009; Moon et al. 2011). Due to mean-state teleconnections, the presence of tropical Pacific biases also affects the mean climate state in remote locations, such as the tropical Atlantic and Indian Oceans, and over continental areas of the Americas, Asia, and Australia.

Much effort has been directed towards diminishing these biases and considerable progress has indeed been made in identifying the multitude of factors that can influence the tropical Pacific (Gent 2010). Many of the factors are local, such as coupled ocean–atmosphere feedbacks (Wood et al. 2011) or biological couplings (Jin et al. 2012), and some are remote, such as clouds (Hwang and Frierson 2013) and ocean heat transport (Frierson et al. 2013).

Previous studies such as Maes et al. (1997), Large et al. (2001), and Pezzi and Richards (2003) suggested that small-scale processes, such as lateral mixing, play an important role in the simulation of the coupled dynamics of equatorial SST and large-scale atmospheric circulation. Errors in model formulation and process parameterizations (Jochum and Potemra 2008; Neale et al. 2008; Jochum 2009; Neale et al. 2013) are frequently implicated and various remedies have been prescribed. However, serious biases still remain in even the best GCMs, such as the NCAR Community Earth System Model (CESM) and its components the Community Atmospheric Model (CAM) and the Parallel Ocean Program model (POP) (Gent et al. 2010).

Many attempts at relieving these biases involve adjusting parameters associated with key processes, such as convection in the atmosphere or mixing in the ocean, and then running the model to equilibrium to determine the new, possibly improved, seasonal mean climate state. But often those types of experiments lead to deterioration in the resulting climate, or improving it in one location but distorting it in another (e.g., Jochum and Potemra 2008; Neale et al. 2008).

### **3. Regional coupled climate models**

Many of the deficiencies of GCMs can be remedied or assuaged by using limited-domain regional coupled climate models (RCCMs), which include higher resolution but also are highly controlled by the boundary condition forcing driven by global or larger-scale models and observations. RCCMs often include coupling to sea ice, ocean waves, biogeochemistry, and ecosystems, and also run in data assimilation mode. RCCMs have been developed primarily to improve weather prediction (e.g., Gustafsson et al. 1998), but given the merit for high-resolution view of ocean–atmosphere processes, they have been increasingly used to study the dynamics of air–sea coupling and regional climate processes and predictability. RCCMs thus fill an important gap in our understanding of the processes simulated between the coarsely resolved coupled models and the high-resolution regional uncoupled atmospheric models (e.g., Tseng et al. 2012).

Use of the same physical parameterizations developed for coarse-resolution models for the high-resolution RCCMs can yield poor simulations. In many regional applications with different resolutions, modifications and tuning of the existing physics for the atmosphere (for deep convection and clouds) and ocean (mixing and eddies) models are necessary. There is a need for the modeling community (both global and regional modelers) to improve physical parameterizations to be more spatially scalable for different grid sizes and universal to different geographical regions (e.g., Palmer 2014; Small et al. 2014).

Recent years have seen the development of several regional coupled ocean–atmosphere models—some including the cryosphere, ocean waves, and bottom sediments—which have been applied in various regions around the globe. We highlight a few of them here.

Seo and Miller et al. (2007) developed the Scripps Coupled Ocean-Atmosphere Regional (SCOAR) model in which the ocean is the Regional Ocean Modeling System (ROMS)

(Shchepetkin and McWilliams 2005, 2009; Haidvogel et al. 2008) and the atmosphere is the Regional Spectral Model (RSM) (Juang et al. 1997). This model has been employed in several studies of ocean–atmosphere interaction in various regions with intense thermal ocean fronts such as in the Kuroshio Extension, where mesoscale eddies were shown to affect the winter precipitation (Putrasahan et al. 2013a) and synoptic extreme rainfall events associated with the African Easterly Waves in the Atlantic ocean (Seo et al. 2008a). Recently SCOAR2, using the Weather Research and Forecasting (WRF) model (Skamarock et al. 2008) instead of RSM, was developed by Seo et al. (2014).

Another example is the Coupled Ocean–Atmosphere–Wave–Sediment Transport (COAWST) system modeling as described in Warner and Sherwood et al. (2008). This modular system allowed advances in the representation of coastal dynamics due to the coupling of oceanic and atmospheric circulation models and waves and sediment transport models (Lesser et al. 2004; Warner and Perlin et al. 2008). The atmospheric model is WRF, the ocean model is the ROMS, the wave model is Simulating Waves Nearshore (SWAN) (Booij et al. 1999) and the model of sediment transport is the Community Sediment Transport Modeling Project (CSTM) (Warner and Sherwood et al. 2008). Some of the ocean–atmosphere applications were made to investigate and forecast the interactions between tropical cyclones and the ocean (Bender and Ginis 2000; Bender et al. 2007; Chen et al. 2007).

The US Navy has developed the Coupled Ocean/Atmosphere Mesoscale Prediction System (COAMPS), which includes air–sea–wave coupling and is used on regional scales for short-term operational forecasts as well as for detailed reanalysis simulations over several seasons in support of observational experiments (e.g., Jensen et al. 2016). In coupled simulations surface fluxes are more consistent with observations (e.g., Jensen et al. 2011) and contain less bias than for uncoupled systems (e.g., Small et al. 2011; Allard et al. 2014). High vertical resolution is needed when coupled to an atmospheric model to capture fresh-water lenses from precipitation and the diurnal cycle during calm conditions. To model the diurnal cycle of SST during the inactive phase of the MJO, a 0.5 m resolution in the upper 10 m was used (Chen et al. 2015; Jensen et al. 2015), and fluxes between the models were exchanged every 6 min using an ESMF coupler. An additional challenge is the formation of high density (cold and saline) water under growing sea ice on the shelf areas in the Arctic. The brine is quickly mixed in the vertical, but is later advected down over the continental margin and contributes to deep water and bottom water formation. The COAMPS ocean component includes processes rarely found in climate models: for instance, diurnal and semidiurnal tides, ocean color prediction, and wetting and drying, which are important on local and regional scales.

#### **4. Key climate processes**

Both global and regional climate models must properly represent many climate processes when attempting to simulate and predict the observed variability of climate. In the context

of precipitation, land–surface coupling and oceanic frontal coupling are two key processes that have recently been the focus of several interesting studies.

*a. Land-surface coupling to the atmosphere*

Land represents a boundary for about 30% of the atmosphere, exchanging with it momentum, energy (radiation and heat), mass (water evaporation and precipitation), and chemical compounds (e.g., carbon dioxide and nitrogen). The land surface processes that underlie the characteristics of the surface runoff and consequent river discharge, on the other hand, determine the interaction between land and ocean (and sea ice).

Land surface states provide interactive boundary conditions to the atmospheric circulation with a high degree of variability, both spatial and temporal. For example, the surface albedo, i.e., the fraction of reflected solar radiation, varies markedly in space, depending on the type of surface cover (e.g., topography, soil type, vegetation type, snow cover). Also the moisture fluxes between atmosphere and land surface exhibit high variability: a dry soil does not provide any moisture source to the atmosphere and, due to its very limited heat capacity, its local thermal response to absorbed solar radiation is considerably high. But a wet soil can exchange moisture even more rapidly than an ocean surface (because of a greater surface roughness), providing to the lower layers of the atmosphere water vapor and energy in the form of latent heat.

These important processes and interactions must be taken into account when modeling the climate system, and, in fact, state-of-the-art climate models include surface components (Sellers et al. 1997; Pitman 2003; van den Hurk et al. 2011). In particular, said in very simple terms, these modules have the task of representing the evolution of the land surface state and account for its interactions with the other components of the climate system. Importantly, the surface energy and water balances are coupled through the evapotranspiration term, which thus emerges as one of the critical parameters of the land surface component, with a key role both in the energy and water cycles. Furthermore, the largest amount of evapotranspiration from land to atmosphere occurs through vegetation, which therefore interlinks the water and biogeochemical cycles (e.g., carbon and nitrogen cycles).

Though a number of processes might contribute to control and influence evapotranspiration, soil moisture, i.e., the amount of water stored in different layers of the unsaturated soil, has a fundamental function. Budyko (1956, 1974) provided a useful conceptual framework, further developed by the recent works of Koster et al. (2004), Seneviratne et al. (2006), and Teuling et al. (2009) (see also Seneviratne et al. 2010 and references therein, for a more complete discussion), where two main evapotranspiration regimes can be defined according to soil moisture availability: an energy-limited regime, where soil moisture exceeds a critical threshold and evapotranspiration is not dependent on its amount; and a soil moisture-limited regime, where soil moisture is below the critical value and its amount provides a first-order constraint to evapotranspiration. When soil moisture, then, drops below a threshold called *wilting point*, the amount of water in the soil is too low and evapotranspiration stops completely. Several recent studies (e.g., Koster et al. 2004; Seneviratne et al. 2006;

Teuling et al. 2006) have shown that this simple conceptual approach provides a representative portrait of the coupling between land and atmosphere and a useful framework for its modeling.

Land surface models (LSMs) describe, among other things, the dependency of evapotranspiration on soil moisture, which acts as a water reservoir for the land surface to provide the overlying atmosphere with water vapor. The evapotranspired water vapor contributes to alter the atmospheric stability, triggering convection and cloud formation, returning eventually to land in form of rainfall. The soil-moisture–precipitation coupling has been extensively investigated in the past decades, with many studies emphasizing the capability of soil moisture to alter the atmospheric boundary layer properties and possibly lead to favorable conditions for precipitation (Betts and Ball 1995; Eltahir 1998; Schär et al. 1999; Seneviratne et al. 2010; Tseng et al. 2016).

Because it regulates the relative distribution of the surface heat flux into latent and sensible heat, soil moisture is one of the drivers of the land–air interface thermal response. This soil-moisture–air-temperature coupling has recently received considerable attention, especially for its possible implication in the occurrence of heat waves (e.g., Fischer and Schar 2009; Miralles et al. 2012).

Though the many diverse links and possible mutual influences between climate and vegetation have been known (or hypothesized) for a long time (e.g., Brovkin 2002 and references therein), only a relatively small number of studies have explored the possible effects of vegetation on climate variability and predictability (Sellers et al. 1996). Particularly, all climate models in the third and fifth phases of the Coupled Model Intercomparison Project (CMIP3 and CMIP5, respectively) using multimodel ensembles (MMEs) of forced greenhouse gases have failed to simulate the patterns or amplitudes of twentieth- and twenty-first-century African drying and rainfall variability (e.g., Xue et al. 2010; Roehrig et al. 2013). These models even yield inconsistent precipitation regarding the signs of future anomalies in the Sahel (IPCC 2007, 2013). After the seminal work of Zeng et al. (1999), which investigated the role of vegetation in the Sahel drought during the 1980s, few studies have been conducted to assess the effects of vegetation distribution (leaf area index, LAI) on potential predictability and prediction skill of GCMs at decadal timescales (Weiss et al. 2012, 2014). The ensemble spread in the trend amplitude remains large in the Sahel (Roehrig et al. 2013). Several modeling studies have suggested that positive feedback resulting from land–surface interactions and the atmosphere can amplify the climate response to forcings such as SSTs or solar variations (Doherty et al. 2000; Tseng et al. 2016). Current projections of climate change in the Sahel are inconclusive, mainly as a result of the large uncertainty of land–atmosphere coupling and the atmospheric response to the ocean (e.g., Cook and Vizy 2006; Douville et al. 2006; IPCC 2013; Tseng et al. 2016). The uncertainty is likely due to the enhanced local wave instability triggered by the largely diverged boundary-layer temperature gradients and amplified by land–atmosphere interactions (Tseng et al. 2016).

*b. Frontal air–sea interaction*

While much of the mid-to-high latitude open ocean is typically driven by the atmosphere (e.g., Cayan 1992), oceanic regions dominated by mesoscale eddies and sharp fronts, such as western boundary currents and the Southern Ocean, tend to drive overlying atmospheric processes (e.g., Pezzi et al. 2004; Minobe et al. 2008; Seo et al. 2008b; Small et al. 2008; O’Neill et al. 2012; Ma et al. 2016). The SST anomalies associated with mesoscale eddies or fronts can modify atmospheric stability, surface wind flow patterns, and precipitation. Indeed many studies have shown ocean–atmosphere coupling over ocean fronts and mesoscale eddies (e.g., Xie 2004; Pezzi et al. 2005; Small et al. 2008; Chelton and Xie 2010); however, the spatial-scale dependence of ocean–atmosphere coupling is not as clear in mid-latitude oceanic fronts, where a strong SST front and mesoscale eddies coexist.

Regional (and even some global) coupled models have been recently used to study the dynamics of this mesoscale/frontal coupled ocean–atmosphere process. Seo and Miller et al. (2007) examined the dynamics of the atmospheric response to SST variability associated with the TIWs and the mesoscale eddies off California. Seo and Jochum et al. (2007) and Seo et al (2008b) subsequently quantified the feedback effect of the atmospheric responses to the energetics of the mesoscale eddies in the tropical Atlantic and Indian Oceans, respectively. Small et al. (2009), using the University of Hawaii regional ocean–atmosphere coupled system (IROAM), demonstrated a significant damping effect of TIW energetics via TIW-induced surface current affecting the surface stress.

A new approach that separates the spatial scale of ocean–atmosphere coupling has been developed by comparing a fully coupled ocean–atmosphere model to the same model with an online 2-D spatial smoother that removes mesoscale SST fields seen by the atmosphere (Putrasahan et al. 2013a,b; Seo et al. 2016; Seo, 2017). The implementation of an interactive 2-D smoother allows large-scale SST coupling to be retained while removing the mesoscale eddy impact on the atmospheric boundary layer (ABL). Putrasahan et al. (2013b) performed a scale-dependence experiment over the Kuroshio Extension region and it revealed that wintertime ocean–atmosphere coupling, represented by the coupling coefficient between wind stress divergence and downwind SST gradients, is significant in both the fully-coupled and interactively smoothed-coupled cases. In fact, the smoothed-coupled case exhibits stronger coupling than the fully coupled case, indicating the presence of a large-scale Kuroshio SST front that maintains large-scale SST anomalies, which in turn influence the ABL. And yet, the largest wind stress divergence anomalies are seen in the fully coupled case, which suggests that mesoscale SST anomalies also have a strong imprint on the ABL. The atmospheric response to the oceanic mesoscale SST was studied by comparing the fully coupled run to an uncoupled atmospheric model forced with smoothed SST prescribed from the coupled run. Precipitation anomalies were found to be forced by surface wind convergence patterns that are driven by mesoscale SST gradients, indicating the importance of the ocean forcing the atmosphere at this scale. Such deep atmospheric response is expected to modify the downstream development of weather systems in the North Pacific, thus potentially affecting the remote circulation (e.g., Seo et al. 2014; Ma et al. 2016).

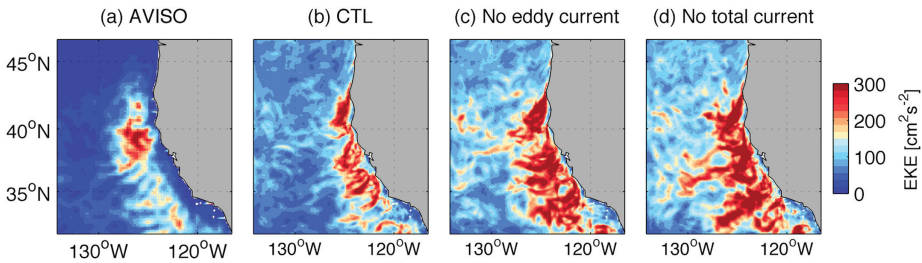


Figure 1. SCOAR model sensitivity simulations showing the impact of air-sea interaction due to SST and surface current on the eddy kinetic energy (EKE). (a) The summertime (July–September, 2005–2010) surface EKE ( $\text{cm}^2 \text{s}^{-2}$ ) derived from the altimeter dataset assuming geostrophy based on the AVISO (Archiving, Validation and Interpretation of Satellite Oceanographic) data. (b), (c), (d) Simulated surface EKEs in a regional coupled model with full coupling (CTL, control experiment), no eddy-current coupling, and no total-current coupling in the wind stress calculations. Adapted from Seo et al. (2016).

In addition to SSTs, the mesoscale eddies produce energetic surface current anomalies, which by creating a velocity shear across the air–sea interface, affect the wind stress and Ekman pumping velocities on oceanic mesoscales. Seo et al. (2016) expanded the 2-D smoothing technique by Putrasahan et al. (2013a) to include the interactive filtering of the eddy-induced surface currents in the California Current System (CCS). They show that the eddy–wind interaction through surface currents leads to remarkably strong dissipation of the eddy kinetic energy (EKE) via reduced momentum input and enhanced surface eddy drag (e.g., Eden and Dietze 2009; Renault et al. 2016). Figure 1 compares the six-year mean summer (June–September) surface EKE per unit mass from a series of regional coupled model experiments. In comparison to EKE from the control simulation (CTL) and from the AVISO sea level anomaly, the coupled run in which the mesoscale surface current effect on wind stress is suppressed produces a considerably (42%) higher EKE (Fig. 1c). When the total ocean current effect is removed, the EKE increased by 53% (Fig. 1d). This indicates that most of the EKE reduction is done by eddies rather than by the background current. This EKE damping mechanism through the eddy–current–wind interactions leads to an improved simulation of the energetics of the CCS.

The interactive smoothing technique paves the way for future studies to help identify the impact of oceanic mesoscale features on the ABL through surface-flux coupling processes in various regions of the world’s ocean, or investigate any rectified response of precipitation to oceanic fronts and eddies (e.g., Taguchi et al. 2009; Xu et al. 2011). This framework can also be used to separate the thermodynamical and dynamical effects of oceanic mesoscale eddies on atmospheric flow and processes, as well as determine any feedback of ocean induced atmospheric anomalies on the ocean eddies themselves.

## 5. Patterns and timescales of climate variability

We next highlight several of the most important regional modes of variability that are linked to precipitation impacts through coupled ocean–atmosphere processes.

### *a. El Niño Southern Oscillation*

The El Niño Southern Oscillation (ENSO) is the largest natural mode of climate variability in the global climate system with wide-ranging teleconnections around the Pacific basin (e.g., Philander 1990). It is generated by coupling between the ocean and the atmosphere in the tropical Pacific that causes small amplitude perturbations to either SST or wind stress to grow in tandem to produce the familiar pattern of mature SST anomalies (Fig. 2a). These SST anomalies are then damped by atmospheric surface fluxes and relaxed back to the climatological ocean state. Theories for ENSO generation are numerous and are reviewed by Wang et al. (2017).

Successive generations of coupled models have produced simulations of ENSO that have gotten better over time. Yet errors and biases that are common to all models exist in both the mean climate and the variability of the tropical Pacific (Bellenger et al. 2014). The equatorial cold tongue is usually too cold and extends too far into the west. Models suffer from the so-called “double ITCZ” problem (Lin 2007) whereby the SPCZ is too zonally oriented. Warm-pool convection is impacted by these biases and is, in general, fragmented and not as organized as convection in the real world. There is a wide diversity of ENSO characteristics in models with differences in amplitude and frequency in comparison with observations. A perennial problem appears in the simulation of skewness. In the real world, El Niño events are generally larger than La Niña events in terms of their SST anomalies. Models tend to simulate a symmetric distribution of anomalies.

One of the big debates in the literature in recent times has been about the existence of different types of ENSO events. The SST anomaly pattern shown in Figure 2a is generally considered to be a “canonical” or “east Pacific” or “cold tongue” event in which the SST anomaly maximum is towards the coast of South America. Some events, however, do not penetrate that far and have been termed “Modoki,” “west Pacific,” or “warm pool” events (Ashok et al. 2007), as shown in Figure 2d. During canonical events, the thermocline deepens significantly in the east and the thermocline feedback is dominant. During Modoki events, the thermocline is less active and processes such as the zonal advection of SST anomalies from the west play a more important role. It is also suggested that Modoki events have become more prevalent after 2000 because of the change of the mean ocean background states and the reduced variability of the coupling system in the tropics (Lee and McPhaden 2010; McPhaden et al. 2011; Hu et al. 2013). However, it has been argued that these are not really distinct modes but more part of a spectrum of behavior (Takahashi et al. 2011; Capotondi et al. 2015). Every ENSO event is different and is generated by a subtly different combination of amplifying and damping processes. Long model historical simulations and future projections show that significant variations in ENSO characteristics are possible on

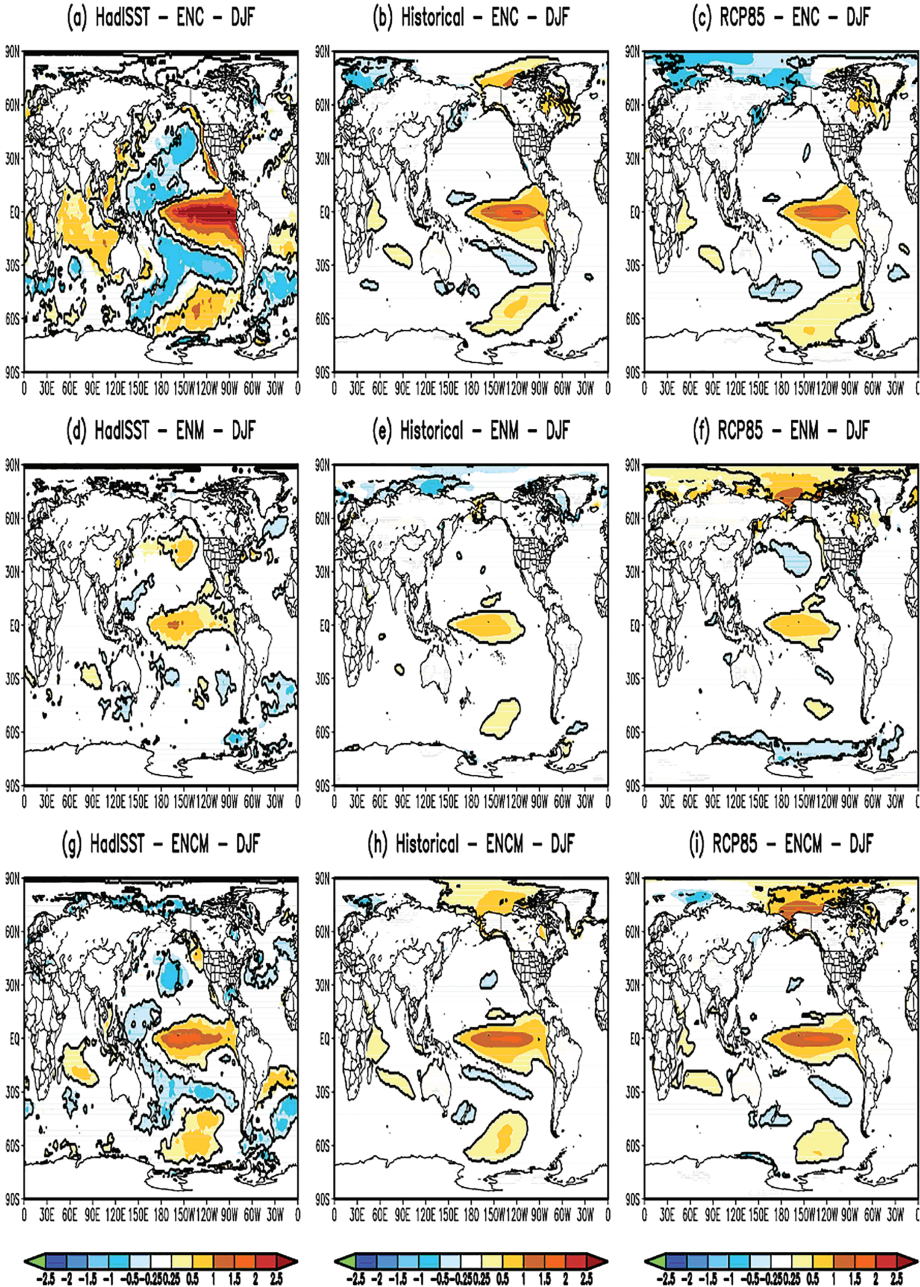


Figure 2. Composite sea surface temperature (SST) anomalies showing the difference between “canonical,” eastern Pacific, El Niño events (top row), the “Modoki” (central Pacific) SST events (middle row), and their combined structure (bottom row). The left column is from the HadISST observational dataset, computed by averaging: (a) 1982–1983 and 1997–1998 El Niño “canonical” events; (d) 1986–1987, 1990–1991, 1994–1995, and 2004–2005 El Niño “Modoki” events; and (g) combined events. The middle column (b, e, h) shows the model representations of those types of (random) events in the historical climate model simulations. The right column (c, f, i) shows them for RCP8.5 model global warming conditions. Adapted from Tedeschi and Collins (2015).

decadal and longer timescales (e.g., Fig. 2, middle and right columns), generated only by natural internal processes in the climate system (Wittenberg 2009; Di Lorenzo et al. 2010; Tedeschi and Collins 2015).

*b. Pacific Decadal Oscillation*

The Pacific Ocean sector exhibits a high degree of decadal variability that impacts the surrounding continents in many ways. One of the most prominent metrics for this variability in the northern region is the Pacific Decadal Oscillation (PDO) index, defined as the leading principal component of sea surface temperature (SST) anomalies north of 20°N in the North Pacific, after adjustment to remove the global SST trend (Mantua et al. 1997; Newman et al. 2016). It is sometimes viewed as an intrinsic part of the larger, Pacific-wide Interdecadal Pacific Oscillation (IPO; Power et al. 1999; Meehl et al. 2013). The PDO is closely associated with forcing by atmospheric pressure fluctuations of the Aleutian Low (e.g., Miller and Schneider 2000). The spatial pattern of SST anomalies associated with the PDO can be seen by regressing the PDO time series onto SST anomalies (Fig. 3a), which reveals a characteristic horseshoe-shaped pattern with warm values in the tropical Pacific, Gulf of Alaska, and along the west coast of North America, and cold values in the central North Pacific. These anomalies are reversed for the negative phase of the PDO.

The time series of the PDO index shows appreciable low-frequency content, with periods when the index is high altering with periods when it is low (Fig. 3b). Considerable research has been focused on the transition between the low and high phases that occurred in 1977. For example, Mantua et al. (1997) found that the 1977 shift was associated with changes in salmon production in the North Pacific. Gedalof and Smith (2001) showed that it affected ecosystems along the west coast of North America; McGowan et al. (2003) showed that it was associated with changes in zooplankton biomass in the California Current system. Yeh et al. (2011) found that the 1977 climate shift differed in some key respects from the later 1988 climate shift. Hare and Mantua (2000) documented an extensive list of physical and ecological changes associated with the 1977 change in the PDO.

The power spectrum of the PDO time series (Fig. 3c) shows the characteristic shape of a first-order autoregressive process (a so-called “red” spectrum), as would be expected from basic physical principles by the ocean continually integrating random perturbations of the atmosphere (Hasselmann 1976; Frankignoul and Hasselmann 1977; see also Pierce 2001). Such red noise processes described by the Hasselmann mechanism are consistent with the regime shifts often described for the PDO, such as the shift in 1977 described above, and it is difficult to find evidence of significant decadal-frequency spectral peaks in the PDO index just using the approximate 100-year observed record of SSTs (Pierce 2001; Newman et al. 2016). This is unlike the ENSO process, which is a coupled ocean–atmosphere mode of interaction that depends on both ocean and atmospheric processes and has a preferred timescale. The PDO is, instead, the result of an amalgam of processes (e.g., Newman et al. 2016) and is not a dynamical mode of variability.

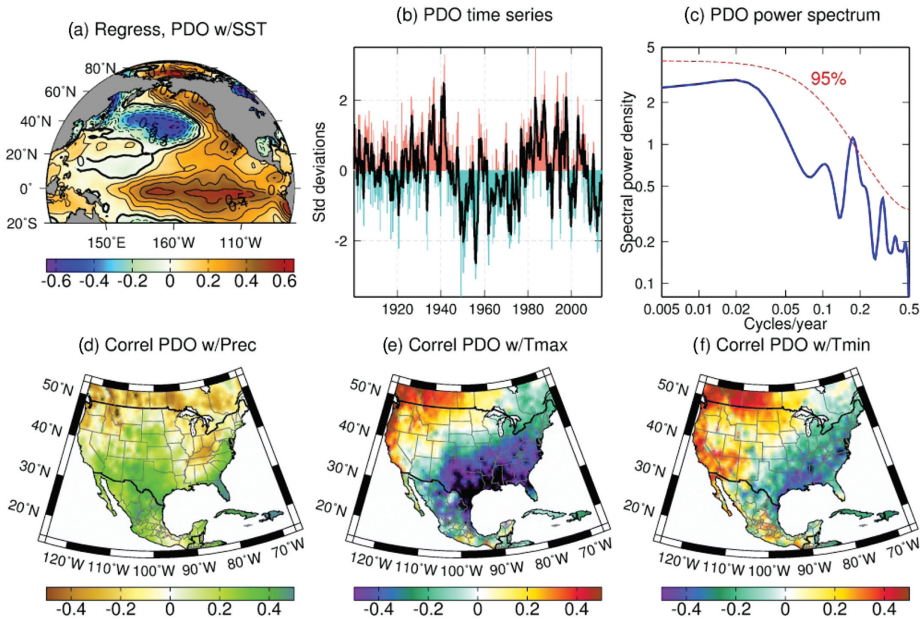


Figure 3. The structure of the Pacific Decadal Oscillation and its effect on winter climate in Mexico and the U.S. (a) Regression ( $\text{deg C}^{-1}/\text{sd}$ ) between the cold season (NDJFM) Pacific Decadal Oscillation (PDO) index and sea surface temperature (SST) anomalies 1946–2014. (b) The PDO time series (Mantua, 2017). Colored bars show the monthly values; the heavy black line shows the seven-year low-pass filtered time series. Values are standardized. (c) Power spectrum of the PDO time series (blue line) along with the 95% significance value assuming the null hypothesis of a first-order autoregressive process (dashed red line). (d) Correlation coefficient between the cold season (NDJFM) PDO index and precipitation. (e), (f) Same as (d), but for daily maximum and minimum temperature, respectively. Meteorological data is from Livneh et al. (2014).

The PDO is associated with changes in precipitation and temperature over land areas adjacent to the North Pacific, including parts of North America (Fig. 3d, e, f). During the high (positive) phase of the PDO, the southwestern and southeastern United States and northern Mexico are wetter than usual, while southern Canada is drier. The Pacific Northwest is warmer than usual, and the southeastern United States colder. The pattern for daily maximum temperature is similar to that for daily minimum temperature, but the two are not identical, which suggests differences in cloudiness associated with the PDO (since clouds influence the diurnal temperature range). The changes in precipitation and temperature affect land ecosystems, and several studies have used paleo tree rings to extend the observational record of the PDO to the era before widespread ocean temperature measurements were available (e.g., Biondi et al. 2001; D’Arrigo et al. 2001; MacDonald and Case 2005). Several studies have found associations between the PDO and climate response over land, such as the PDO

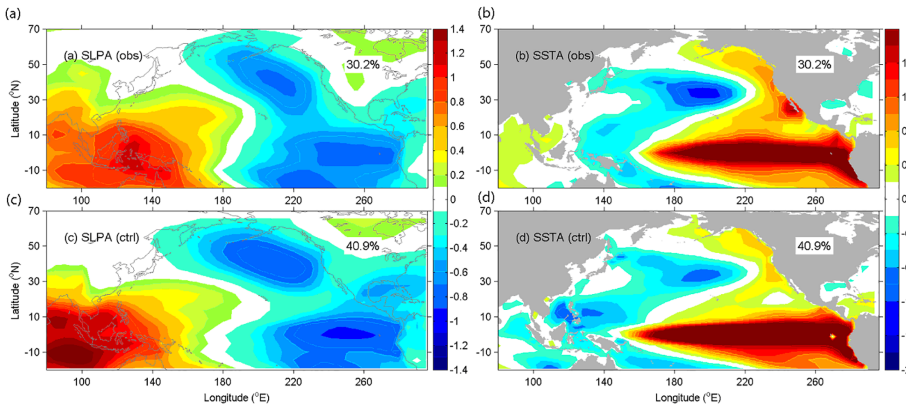


Figure 4. The leading Combined Empirical Orthogonal Function mode (CEOF1) of (a, c) sea level pressure (SLP) anomalies (mbars) and (b, d) sea surface temperature (SST) anomalies ( $^{\circ}\text{C}$ ) (three-month running mean) in the North Pacific (a, b: observation; c, d: the NCAR Community Earth System Model simulation).

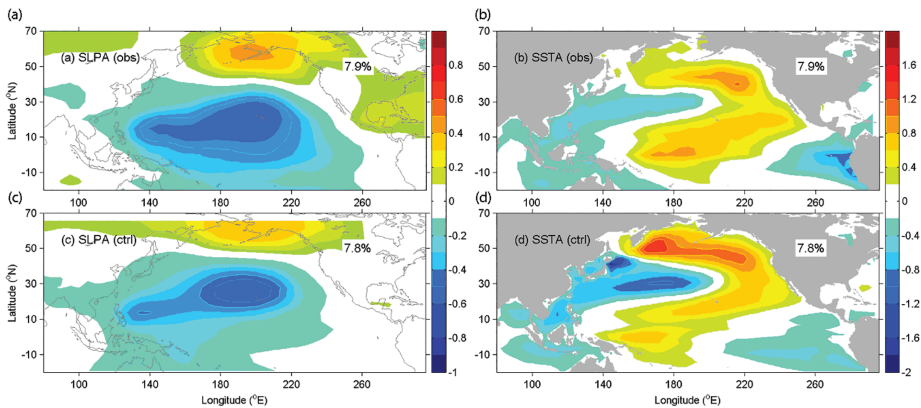


Figure 5. The second Combined Empirical Orthogonal Function mode (CEOF2) of (a, c) sea level pressure (SLP) anomalies (mbars) and (b, d) sea surface temperature (SST) anomalies ( $^{\circ}\text{C}$ ) (three-month running mean) in the North Pacific (a, b: observation; c, d: the NCAR Community Earth System Model simulation).

modulating the effects of ENSO both over North America (Gershunov and Barnett 1998; DeFlorio et al. 2013) and in east Asia (e.g., L. Wang et al. 2008).

Most GCMs are capable of simulating the PDO in their natural variations. For example, Figures 4 and 5 compare the two leading Combined Empirical Orthogonal Function (CEOF) modes of the sea level pressure (SLP) and sea surface temperature (SST) in the observation (top) and CESM version 1 (bottom; Gent et al. 2011). Both the observations and CESM indicate the leading CEOF mode (CEOF1) of SLP anomalies in the North Pacific

is the Aleutian Low (AL), the semi-permanent low-pressure winter center over the Aleutian Islands caused by planetary waves, in association with another strong pressure high near the Indo-Pacific warm pool region and another strong pressure low near the eastern tropic. The canonical PDO/ENSO pattern emerges in the CEOF1 of SST anomalies (Fig. 4b and 4d). The second CEOF mode (CEOF2) of SLP anomalies in the North Pacific (Fig. 5) represents a meridional dipole structure of the North Pacific Oscillation (NPO) in the central-eastern Pacific. In addition, the CEOF2 of the SST footprint resembles the North Pacific Gyre Oscillation (Di Lorenzo et al. 2008), another prominent mode of Pacific decadal variability.

GCM experiments also show, however, that a PDO-like signal is present in the atmosphere even when SSTs are fixed, indicating the primary role of intrinsic atmospheric fluctuations in forcing the PDO. The amplitude of the PDO increases when an oceanic mixed layer model is added under the atmosphere, and increases again when full ocean dynamics are added, especially in the decadal frequency range (Barnett et al. 1999; Pierce 2001). Different oceanic processes contribute to enhanced power at different frequencies and locations (e.g., Schneider et al. 2002; Miller et al. 2004; Schneider and Cornuelle 2005). Part of this increase in North Pacific variability due to ocean dynamics can be ascribed to ENSO, which creates a teleconnected response through the atmosphere that contributes to ocean variability in the North Pacific (e.g., Alexander et al. 2002; Newman et al. 2003; Deser et al. 2004). This likely accounts for the spectral peak at near ENSO timescales in Figure 3c, and may partially explain the similarities between the effects of the PDO and ENSO on North American precipitation and temperature (Fig. 3d, e, f).

Multiple observational reconstructions of equatorial trade winds and wind stress seem to indicate highly anomalous strengthening over the past one to two decades (Fig. 6), potentially outside the range of natural variability in terms of its magnitude and longevity. While this has been attributed to a negative phase of the PDO, the PDO index indicates that the recent negative phase is not anomalous in the historical record. Notwithstanding this, the association of a negative PDO with the enhanced trades is not, in itself, an explanation, as we do not possess a complete dynamical description of the PDO as a self-contained mode of variability (in comparison with the ENSO case in which there are plausible dynamical descriptions). The strengthening trades are of the opposite sign to that which is expected under climate change theory, which predicts a weakening due to the sub-Clausius-Clapeyron response of global precipitation (Held and Soden 2006; Vecchi et al. 2006). Farneti et al. (2014) recently suggested a tropical–extratropical, ocean–atmosphere coupled mechanism to drive the Pacific interdecadal variability and, specifically, lead to the recent enhanced trade winds. The coupled mechanism links the changes in atmospheric circulation directly with the Pacific subtropical cells (STCs) variability on multidecadal timescales. It has been shown that Pacific STCs are directly connected with the interannual ENSO variability (Chen et al. 2015). Unfortunately, our understanding of the STCs, and their decadal to multidecadal variability in relation to the surface wind stress, remains limited due to the lack of observational data and model simulations.

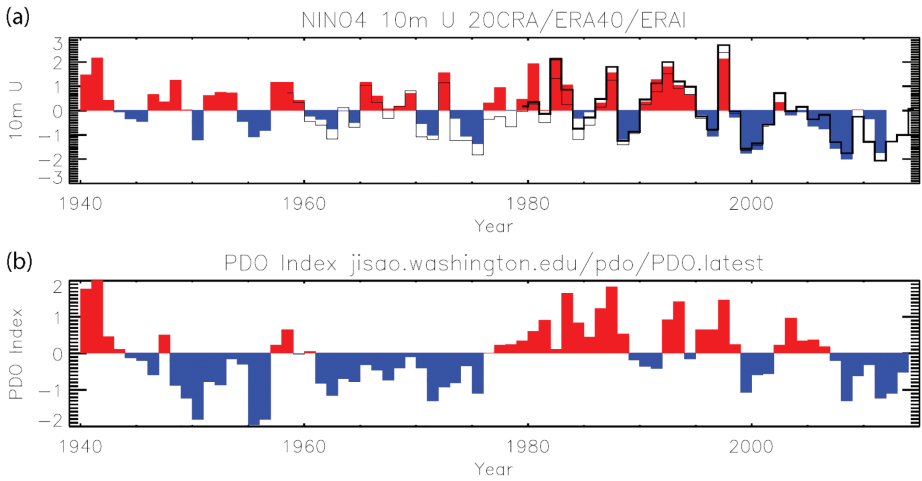


Figure 6. Time series from 1940–2014 reveal a general association of negative PDO phases with enhanced trade winds. (a) An estimate of the strength of the zonal component of the trade winds (10 m zonal wind velocity) annually averaged in the NINO4 box ( $160^{\circ}\text{E}$ – $150^{\circ}\text{W}$ ,  $5^{\circ}\text{S}$ – $5^{\circ}\text{N}$ ) from three different reanalysis products—the 20th Century Reanalysis (Compo et al. 2011), colored bars; ERA40 (Uppala et al. 2005), thin black line; and ERA Interim (Dee et al. 2011), thick black line. (b) An annual-average index of the Pacific Decadal Oscillation (Mantua et al. 1997) formed from the time component of the leading empirical orthogonal function of sea surface temperatures in the North Pacific. In each panel anomalies are computed for 1979–2014 (the period of the shortest time series).

There is mounting evidence that the Pacific has played a leading role in the global warming hiatus observed in the last 15 years or so (Kosaka and Xie 2013; England et al. 2014; Watanabe et al. 2014; Amaya et al. 2015; Roberts et al. 2015)—an event which has been widely discussed within the scientific community and on the global geopolitical stage. The stronger trade winds drive enhanced upwelling of cold waters in the east Pacific that cool the SSTs, but also potentially drive enhanced sensible and latent heat fluxes which may have contributed to the observed cooling. The enhanced upwelling is part of the STCs system that accelerates due to an enhanced off-equatorial wind stress curl. This acceleration subducts warm subtropical water from off the equator into the thermocline in the west, similar to the recharge phase in the ENSO cycle. It is worthy of note that global warming has apparently rebounded after 2015, supporting the multidecadal variation in the Pacific ocean–atmosphere coupling proposed in Farneti et al. (2014).

### c. Atlantic Meridional Overturning Circulation

The Atlantic Meridional Overturning Circulation (AMOC) has been long believed to be a key component of the decadal and longer timescale climate variability, characterized mainly by a warm and saline northward water in the upper layers of the Atlantic (above 1000 m) to supply the formation of North Atlantic Deep Water (NADW) in the Nordic and

Labrador Seas, which returns southward in the deep Atlantic (approximately 1500–4500 m). The other weaker component in the AMOC is the Antarctic Bottom Waters flowing northward below 4500 m and rising into the lower part of the southward-flowing NADW. A substantial amount of heat is transported from the tropics and southern hemisphere toward the North Atlantic in the ocean, where the heat is released to the atmosphere at high latitudes. Since the AMOC carries a significant amount of heat, resulting in the change of Atlantic sea surface temperature, it has a profound impact on the global climate system, as indicated by observations and models (e.g., Clark et al. 2002; McManus et al. 2004; Sutton and Hodson 2005; Hurrell et al. 2006; Lynch-Stieglitz et al. 2007, 2011). Any slowdown in the overturning circulation would have potential implications for a “collapse” or an abrupt change of climate (Rind et al. 2001; Hall et al. 2006; Stouffer et al. 2006; Thornalley et al. 2010; Hawkins et al. 2011).

It has been well recognized that AMOC variability is closely linked with the change of subpolar gyre (SPG, defined here as 60°W–10°W, 50°N–66°N), particularly the decadal variability of the North Atlantic SST (e.g., Häkkinen and Rhines 2004; Böning et al. 2006; Bersch et al. 2007; Rhein et al. 2011). The SPG is known as the deep water formation region (resulting mainly from the deep convection in the Labrador Sea) of the intermediate water mass due to intense air–sea interaction, especially during severe winters (Dickson et al. 1996; Lab Sea Group 1998).

However, how the AMOC is connected with the atmospheric circulation is still not clear. Previous studies have suggested that the North Atlantic Oscillation (NAO) variability significantly contributes to the oceanic variability in the North Atlantic SST pattern and circulation (Eden and Willebrand 2001; Visbeck et al. 2003; Deshayes and Frankignoul 2008). The influence of NAO on the Atlantic Multidecadal Oscillation (AMO) has been discussed extensively in numerical model studies (e.g., Delworth et al. 1993; Visbeck et al. 1998; Delworth and Greatbatch 2000; Eden and Jung 2001; Eden and Greatbatch 2003; Danabasoglu et al. 2012). Substantial modeling evidence has confirmed that the NAO-related surface turbulent heat flux anomalies over the North Atlantic, particularly over the SPG, influence the multidecadal variation of the AMOC, which in turn produces the SST signatures of the AMO and the interannual and longer timescale sea-surface height (SSH) variability in the North Atlantic (Esselborn and Eden 2001; Häkkinen 2001; Volkov and van Aken 2003; Yeager and Danabasoglu 2014). Thus, the AMO may be a delayed response to low-frequency NAO variability at time lag of decadal timescales (Visbeck et al. 1998; Delworth and Greatbatch 2000; Eden and Jung 2001; Lohmann et al. 2009) in the response of the AMOC change (as indicated by the Atlantic dipole) through the changes in Labrador Sea convection (Wood et al. 1999; Hillaire-Marcel et al. 2001; Latif et al. 2006).

Similarly, using numerical models, the low frequency SSH variability along the Gulf Stream and in the SPG is related to the meridional overturning (Häkkinen 2001). Zhang (2008) further suggested that the pattern of SSHa could be used as a “fingerprint” of the AMOC variations in the mid-to-high latitudes using a 1000-year model simulation.

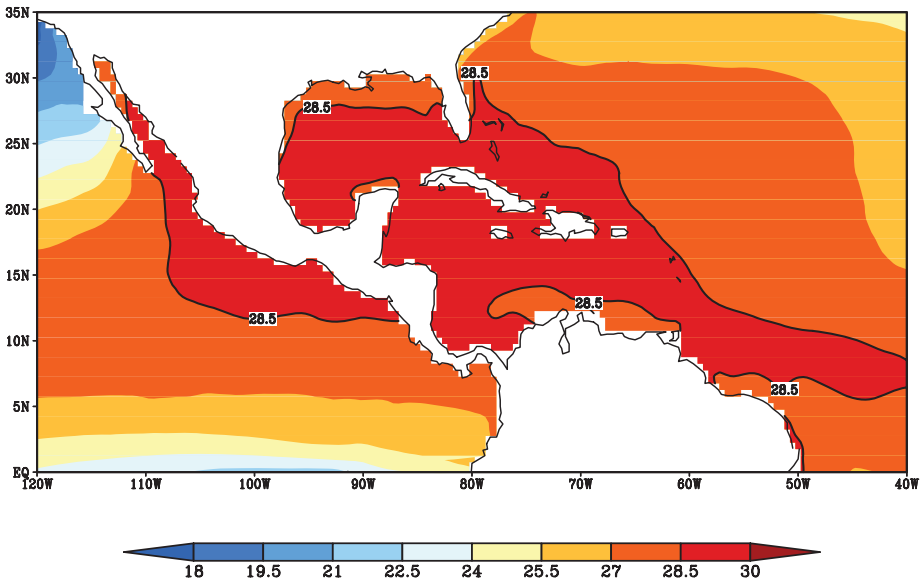


Figure 7. Climatological distribution of sea surface temperature during the peak August–September–October season of Atlantic Warm Pool. The area enclosed by 28.5°C is contoured, which defines the Western Hemisphere Warm Pool and the Atlantic Warm Pool.

However, caution is warranted in representing the AMOC change using SSHa given the existence of a high-frequency wind-driven response as suggested by Lorbacher et al. (2010).

## 6. Regional examples

We next examine two key examples of coupled ocean–land–atmosphere interactions that affect the precipitation in specific regions of the world.

### a. Intra-American Seas

The Intra-American Seas (IAS) comprises the Gulf of Mexico, Caribbean Sea, and parts of the northwestern tropical Atlantic Ocean. It hosts the largest pool of warm water ( $\geq 28^\circ\text{C}$ ) in the western hemisphere besides a small adjacent region in the northeastern tropical Pacific Ocean (Fig. 7). This large pool of warm water, which appears in midboreal summer season and disappears by late boreal fall season is termed the Western Hemisphere Warm Pool (WHWP; Wang and Enfield 2001). C. Wang et al. (2008) suggest that the WHWP is more strongly influenced by the variability of the area of the warm pool in the Atlantic Ocean, which is much larger in area than its counterpart in the northeastern tropical Pacific. This Atlantic Warm Pool (AWP) is objectively defined by the area enclosed by the 28.5°C isotherm in the IAS region (Fig. 7). The AWP displays a very strong seasonal cycle, with the AWP area peaking in August–September–October (ASO) season. This allows, following Misra et al. (2014), objective definition of the onset of the AWP season based on the first day

when the daily area of the AWP exceeds the climatological annual mean area of the AWP. Similarly, the demise of the AWP season is defined as the first day after the onset of the AWP season when the daily area of the AWP falls below the climatological annual mean area of the AWP. Based on these definitions, Misra et al. (2014) indicate that the climatological onset date of AWP is June 21 and the climatological demise date is November 5. A rich literature of observational studies indicate that the AWP undergoes frequency modulation on several timescales that produces atmospheric teleconnections including at intraseasonal (30–50 days; Maloney and Hartmann 2000; Higgins and Shi 2001), seasonal (Wang and Enfield 2003), interannual (Wang and Enfield 2001; C. Wang et al. 2006; Misra et al. 2009), and decadal (Wang et al. 2008) timescales.

The variability of the AWP has been associated with corresponding warm season variations of North American precipitation cycles (C. Wang et al. 2006, 2008; Misra et al. 2011, 2014; Misra and DiNapoli 2013). A primary aspect of this influence stems from the modulation of the low-level atmospheric flow (Fig. 8a), which includes the modulation of the North American subtropical high, more prominently referred as the Bermuda high. In years of large (small) AWP, the Bermuda high becomes weaker (stronger) and extends to the east (west), which leads to anomalous low-level northerly (southerly) flow over the central Plains and Mississippi and Ohio River valleys. This anomalous flow suggests the weakening (strengthening) of the North American low-level jet along the eastern slopes of the Rocky Mountains, which disfavors (favors) moisture transport into the central United States that results in dry (wet) ASO seasonal rainfall anomaly (Fig. 8b). On the other hand, the low level easterly flow in the Caribbean Sea and the eastern Pacific is also modulated by the AWP variations, which effectively influences the moisture flux convergence over Central America in such a way to increase (decrease) the ASO seasonal mean rainfall during large (small) AWP years. The interannual variation of the AWP and its teleconnection with the low level flow (Fig. 8a) and the associated rainfall anomaly (Fig. 8b) over North America is found to be independent of the El Niño and the Southern Oscillation (ENSO) variation (Wang and Enfield 2003; Misra et al. 2013).

AWP variations also have an impact on the Atlantic hurricane season, with large (small) AWP years producing the likelihood of more (less) Atlantic tropical cyclones (Wang et al. 2006). For example, in 18 years of large (18 years of small) AWP between 1950 and 2003, there were 11 (3) active Atlantic hurricane seasons with a total of 82 (23) tropical storms. This influence of the AWP is largely from its modulation of the vertical wind shear in the tropical Atlantic (Wang et al. 2006). The AWP variations not only modulate the low-level flow but also the upper level atmospheric circulation as the anomalous diabatic heat release in the IAS elicits a “Gill” type response (C. Wang et al. 2008; Lee et al. 2009), which affects the large-scale wind shear in the tropical Atlantic Ocean.

Surface heat budget studies in the IAS reveal that cloud-radiative fluxes, especially those which relate to longwave cloud radiative feedback, are some of the most important terms to regulate the SST in the AWP region (Wang and Enfield 2001; Misra et al. 2013). Although the contribution to the SST variability in the IAS region during the AWP season from

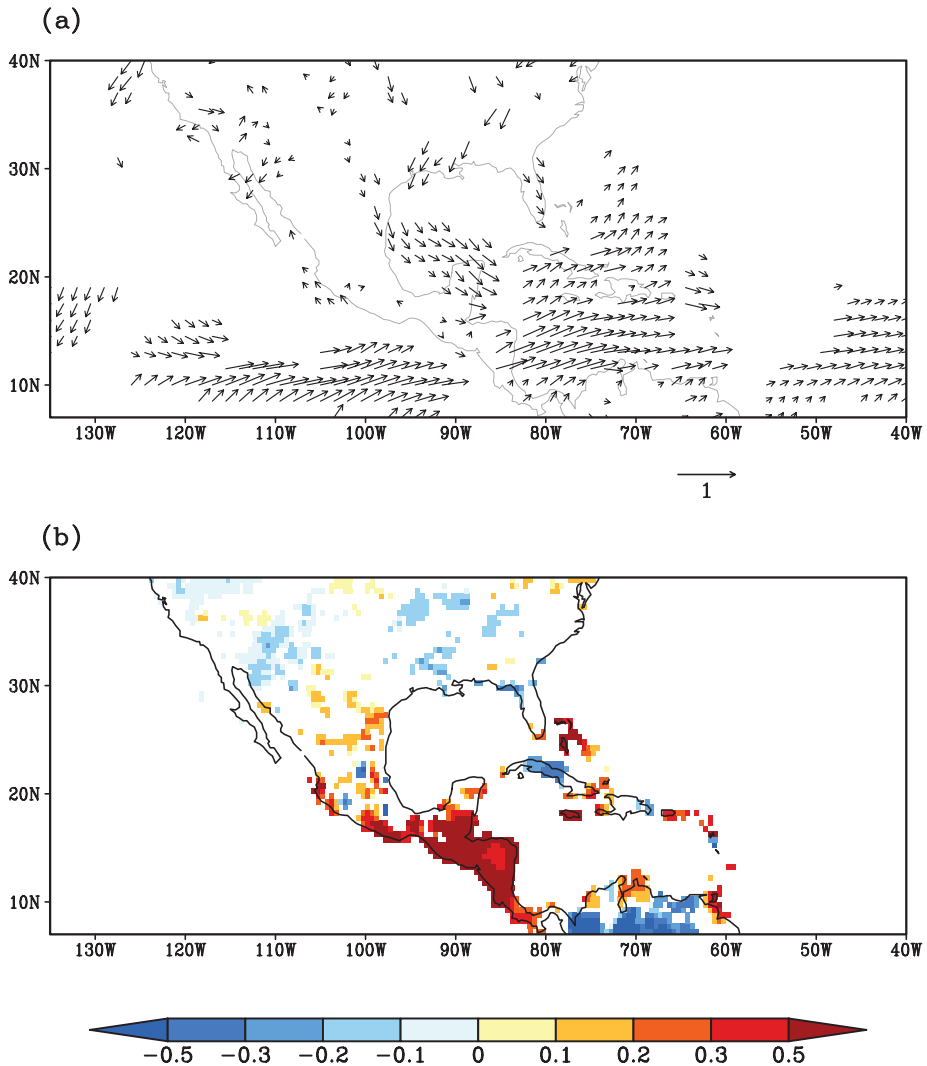


Figure 8. The regression of August–September–October (ASO) seasonal mean (a) 850-hPa wind flow from Climate Forecast System Reanalysis (Saha et al. 2010) and (b) Climate Prediction Center merged precipitation analysis (Chen et al. 2008) on the corresponding seasonal ASO Atlantic Warm Pool area anomaly. Only significant values at 90% confidence interval according to t-test are shown. The period 1982–2010 was used in this analysis.

oceanic advective terms is relatively small, it should be recognized that they play a vital role in sustaining warm pools (Clement et al. 2001). In the case of the IAS, the loop current through the Yucatan Channel is a vital source of transporting heat from the deep tropical Atlantic to the subtropical Gulf of Mexico.

The global models of the CMIP class (both the CMIP3 and CMIP5 suites) display a very cold bias, thereby underestimating the AWP by a very large margin (Misra et al. 2009; Kozar and Misra 2012; Liu et al. 2012, 2013). Liu et al. (2012) find that when observed SST forces an atmospheric GCM then excessive precipitation is generated over the AWP region during the summer, contrary to observations. They further find that when the atmosphere and ocean models are fully coupled, there is a dry and cold SST bias in the AWP region. The cause of these model biases in the AWP region is a challenging problem, although it has been suggested that the largest impact on the rainfall bias over North America in the boreal summer and fall seasons may come from the negative SST biases, since the same CMIP3 models that have the least SST bias in the IAS region also have the most realistic rainfall (Liu et al. 2012).

### *b. Mediterranean basin*

The Mediterranean region has been identified as one of the most responsive to climate change (Giorgi 2006; Diffenbaugh and Giorgi 2012), and being also densely populated (more than 500 million people live here, distributed over approximately 30 countries in Africa, Asia and Europe), it represents one of the most interesting case studies from the scientific point of view and is important from a social perspective (Navarra and Tubiana 2013).

Via atmospheric teleconnections, the variability at intraseasonal and interannual timescales in the area is strongly influenced by the major large-scale circulation patterns of the Northern Hemisphere, such as the North Atlantic Oscillation, the East Atlantic pattern and the Scandinavian pattern (see Ulbrich et al. 2012 and references therein for an extensive review). Tropical variability, especially ENSO (Mariotti et al. 2002; Alpert et al. 2006), the South Asian monsoon (Rodwell and Hoskins 1996; Ziv et al. 2004) and the West African monsoon (Alpert et al. 2006) also appears to exert some influence on the Mediterranean region.

The atmospheric circulation patterns associated with large-scale modes of variability (e.g., NAO, AMO, or ENSO) are modulated by the small-scale processes induced by the local complex physiography of the region (e.g., orography and land-sea contrast). The small-scale events resulting from this interaction have important effects in forcing the Mediterranean Sea circulation, which, in turn, can feedback on the atmosphere providing moisture and heat, as, for example, seems to happen in the case of the Mediterranean cyclones.

Decadal and multidecadal variations in regional precipitation, surface air temperature, and Mediterranean SSTs have been documented and investigated in numerous studies (e.g., Hurrell et al. 2003, Xoplaki et al. 2004; Mariotti and Dell'Aquila 2012). Specifically focusing on the major drivers of decadal and multidecadal Mediterranean climate variations in northern winter (DJF) and summer (JJA) seasons, these studies have shown that precipitation variations over large portion of the region are significantly affected by the low-frequency variability of the North Atlantic Oscillation via modifications in sea level pressure and associated circulation anomalies.

In general, GCMs (e.g., CMIP3 and CMIP5) can reproduce some basic large-scale features of the observed Mediterranean climate (e.g., Kelley et al. 2012; Baker and Huang 2014), even if substantial biases appear to persist (e.g., Cattiaux et al. 2015). However, due to their limited spatial resolution, global models clearly fail in reproducing the small-scale processes and circulation features described above and that appear to be important elements of the regional climate. Marcos and Tsimplis (2008), for example, showed that CMIP3 general circulation models reveal many difficulties in simulating a realistic Mediterranean Sea temperature and salinity in present climate, most likely because of their low resolution. Similarly, Elguindi et al. (2009) showed that global models have too coarse resolution to correctly describe heat and momentum air–sea fluxes over the basin. These problems, in turn, reflect on the lack of ability of global models to reproduce a realistic climatology and variability of the Mediterranean cyclones (Flaounas et al. 2013) and associated precipitation (Sanna et al. 2013).

In the framework of the EU project CIRCE (Climate Change and Impact Research: The Mediterranean Environment; Navarra and Tubiana 2013), a set of coupled atmosphere–ocean models have been developed with the aim of producing climate change projections for the Mediterranean region (Gualdi et al. 2013). Following Somot et al. (2008), all of the models were composed by a relatively high-resolution atmospheric component (ranging from about 80 to about 25 km) fully coupled with a high-resolution numerical model of the Mediterranean Sea (from about 12 to about 7 km), which allowed resolving the small-scale dynamical features of the basin. Compared to the climate models commonly used to perform climate (scenario) simulations for the Euro-Mediterranean area, the major novelty featured by the CIRCE models was the inclusion of a fully interactive, mesoscale-permitting Mediterranean Sea into the climate system.

With these models, the evolution of some key variable (e.g., SST, sea level, water and heat fluxes) is simulated with a high degree of physical consistency due to coherent, high-resolution air–sea flux modelling and well-resolved physiographic features of the basin. When compared with the results obtained with global low-resolution models (e.g., Coupled Model Intercomparison Project, CMIP3), the CIRCE simulations show some improvement in reproducing the seasonal means of T2m, precipitation, and SST, though substantial systematic errors in near-surface temperature and precipitation continue to occur (Gualdi et al. 2013). Overall, the regional coupled models appear to provide reasonably good estimates of the Mediterranean surface water budget and heat budget, which are generally in better agreement with observations compared to the results obtained with atmosphere only models (Dubois et al. 2012).

## **7. Issues of predictability, predictions, and projections**

In this section, we discuss a variety of issues related to the theoretical predictability, practical predictions, and multidecadal-scale projections under global warming scenarios of the various modes, particular regions, and climate processes presented above. We emphasize

that the prediction of anomalous climate states of climate modes of *natural variability* have temporal limits due to inherent nonlinearities in the climate system. These limits of predictability are currently an active line of study for many research groups around the world. The *forced signal* due to increasing greenhouse gases, in contrast, rises further above the climate noise the further into the future the predictions are made because of the increase in signal-to-noise ratio. It provides a measure of changes in the mean state and variance levels of the climate system and forms the basis of IPCC projections. In the near term, the prediction problem is a mixed initial condition/boundary condition problem with, in general, the signal coming from the initial state in the first few years–decades and the signal coming from the forcing climate change response growing in time. Studies have attempted to partition the uncertainty in predictions along these lines. There is a natural definition of near-term as being when the forced response does not depend on the scenario.

The sensitivity of model forecasts of climate variables, such as precipitation, to model initial conditions and different parameterization lead to uncertainty in single model forecasts, making the use of ensemble forecasts necessary to reduce forecast errors and to provide an estimate of the errors. For ensembles of fully coupled models the required computing resources are onerous and generally only able to be carried out by national centers of climate prediction. Currently, typical climate model forecasts are initialized from separately analyzed atmospheric and oceanic states, constrained by observations. Data assimilation in the coupled system is an ongoing major research goal in our field and will involve covariance calculation of variables between the submodels, e.g., correlations between atmospheric and ocean observations.

The possibility to perform climate predictions, i.e., to forecast the state of the climate system in the future on the basis of our knowledge of its state at the present, is based on processes that, in their evolution, bring memory of the initial state. The slowly evolving ocean—its large thermal inertia and its dynamics, for example—introduce memory in the system on a broad range of timescales, ranging from subseasonal to decadal and further. This memory is at the basis of the predictability of several processes and of our skill to predict them; for example, as in the case of the ENSO fluctuations on interannual timescales and, to a lesser extent, for the interannual and decadal fluctuations of the North Atlantic and North Pacific SST (e.g., Schneider and Miller 2001; Boer 2011; Doblas-Reyes et al. 2013). Temporary heat storage by the ocean may also be important in causing decadal variations in global mean temperature such as the recent hiatus in global warming.

Efforts for understanding regional climate processes using RCCMs are leading to developing and examining regional climate change scenarios using projection and uncertainty information from GCMs, in which key oceanic and coastal processes are poorly captured. GCM predictions are typically generated on a grid in which numerous observed data points are available, thereby providing multiple ways to validate forecasts. In contrast, regional coupled climate models have far more grid points than available data; because of the lack of a sufficient quantity of point measurements in nature compared to the density of model gridpoints, it is often difficult to evaluate the downscaled fields of regional models and to

quantify uncertainties (or errors). In regional atmospheric and ocean models, the downscaled skill is impacted by multiple factors including the large-scale fields via lateral boundary conditions, the domain size, inconsistencies of the physics used in the nested and parent models, and finally the internal variability arising from the coupled system. RCCMs predict the SST; land surface conditions; and surface ocean–atmosphere heat, moisture and momentum fluxes; as opposed to them being specified in RAMs and ROMs. Because of this air–sea coupling and uncertainty in prediction, internal variability of the coupled model can be amplified, increasing discrepancy of the interior solutions with the lateral boundary conditions and thus contributing to biases and forecast errors. Ensembles of RCCM predictions are useful to distinguish the physical response more reliably versus internal variability of the coupled system interacting with the prescribed, forecasted boundary conditions.

The processes underpinning land–atmosphere interaction, in particular the coupling between temperature, soil moisture and precipitation, might potentially increase the predictability of the climate system by transferring the information of surface state anomalies to the atmosphere at different timescales. Since the pioneering and seminal works of Shukla and Mintz (1982) and Fennessy and Shukla (1999), a number of studies have explored the potential of soil moisture for seasonal climate predictability (e.g., Koster et al. 2004; Ferranti and Viterbo 2006; Douville 2010; Paolino et al. 2012; Materia et al. 2014). The results indicate that moisture anomalies in the soil may persist for months, determining a land surface memory, which in some areas contributes to an increase in the seasonal predictability (Douville 2010; Paolino et al. 2012; Materia et al. 2014).

The potential influence of land surface processes on climate predictability at timescales longer than the seasonal is a matter of very recent development (for a review, see Bellucci et al. 2015). Information from the slow varying components of the land surface system, such as, for example, ground water and especially vegetation, might lead to enhanced predictability at interannual or longer timescales. Evapotranspiration from land to atmosphere occurs mostly through vegetation, and thus changes in the vegetation characteristics (e.g., distribution) might have substantial influences on the evolution of the climate system.

In the Pacific sector, a great deal of attention has been directed towards determining whether the climate processes associated with the PDO are predictable. Numerical experiments with a single coupled climate model (CCSM4) show that initializing the ocean to the pre-1977 thermal structure and then letting the model evolve forward in time results in a reasonably accurate prediction of the 1977 climate shift (Meehl and Teng, 2012), so some part of the decadal variability might be predictable, at least in the ocean. However, a wider selection of seven climate models showed a large spread in model ability to predict the PDO, and overall the models showed less predictive skill than could be found by assuming simple persistence (Kim et al. 2012). It is worth noting that for a pure first-order autoregressive process no predictability exists except for persistence. However more work needs to be done to understand whether the differences among models are due to sampling variability or poor model representations of the key physical processes, which might be negatively affecting the ocean predictability results.

The potential for using the PDO to predict climate variations over land is less clear, despite the associations illustrated in Figure 2d, e, f. Numerical experiments suggest that specifying PDO SST patterns as lower boundary conditions to an atmospheric model has little subsequent effect downstream (Pierce 2002; Kumar et al. 2013). Several studies have found associations between the PDO and climate response over land, such as the PDO modulating the effects of ENSO both over North America (Gershunov and Barnett 1998) and in east Asia (e.g., L. Wang et al. 2008). However, the degree to which these effects arise from more than simple persistence of the PDO, or the ocean merely passively recording atmospheric states that are the ultimate cause of the land effects, is not clear; more research on this topic is needed (Newman et al. 2016). The exception might be in coastal regions immediately adjacent to the North Pacific, where land temperatures are directly influenced by ocean temperatures. For instance, Alfaro et al. (2004) show that up to a third of the variance in coastal California summer air temperatures can be predicted one season ahead using the PDO.

Future changes in the PDO due to anthropogenic forcing of the climate have not been extensively studied. Furtado et al. (2011), examining the older generation of climate models, show no clear future model consensus on PDO changes. However, the models generally did not capture current relationships between PDO and ENSO in the first place, which casts doubt on their ability to predict future changes. Di Lorenzo et al. (2010), by contrast, focus on the North Pacific Gyre Oscillation (NPGO) rather than the PDO, and conclude that the NPGO is relatively more sensitive to ENSO variability in the central tropical Pacific than is the PDO. Since it is thought that central Pacific ENSO events may increase in the future (Yeh et al. 2009), changes in the NPGO may be relatively more important to future climate than changes in the PDO. Considerably more work remains to be done to understand this issue.

Year-to-year ENSO variability is controlled by a delicate balance of amplifying and damping feedbacks and the physical processes that are responsible for determining the characteristics of ENSO will be modified by climate change (Collins et al. 2010). Recent studies have suggested an increase in the frequency of extreme ENSO events under climate change (Cai et al. 2014, 2015) as shown in Figure 9. This increasing frequency is linked to an enhanced and nonlinear precipitation response (Power et al. 2013; Chung et al. 2014), but this precipitation response is not seen in simulations in which uniform SSTs are imposed. Models show an increase in the central and east Pacific, anchored to a pattern of equatorially enhanced SST changes (Xie et al. 2010). The pattern of mean SST change is of leading-order importance in determining changes in variability. The whole storyline of increasing extreme ENSO events is thrown into doubt when one considers that long-standing biases in models might influence the mean pattern of SST and precipitation changes in models. Hence there is still considerable uncertainty over how ENSO might change in the future.

In the Atlantic sector, early potential predictability studies showed some possibility of interannual to decadal predictability, in particular in the North Atlantic but with not much

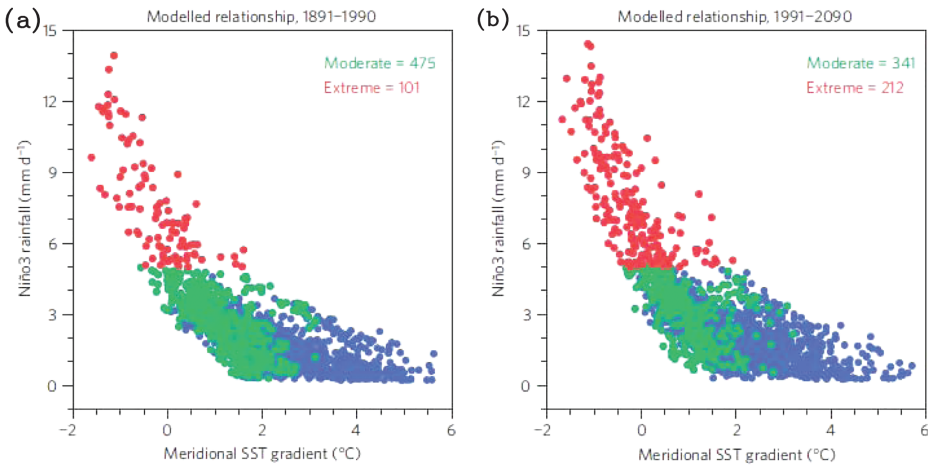


Figure 9. Changes in extreme El Niño events due to global warming simulated in climate models from Cai et al. (2014). Tropical Pacific meridional sea surface temperature (SST) gradient plotted against rainfall in Niño3 area (5°S–5°N, 150°W–90°W) from (a) historical simulations, 1891–1990 and (b) climate change scenario runs, 1991–2090. Red dots indicate extreme El Niño events, green dots indicate moderate El Niño events and blue dots indicate non-El Niño conditions.

predictability of land. A recent study has performed perfect ensembles to look at sea-ice predictability on interannual timescales and found potential signals out to three years. CMIP5 provided the first coordinated set of decadal prediction experiments but little has been found from those studies as (i) many of the systems were experimental and (ii) the design of the experiments was not perfect. The experiments had insufficient start dates to assess skill and included volcanic aerosols, which are unpredictable in real-time, in the forcing files. As one example, Doblas-Reyes et al. (2013) executed retrospective decadal forecasts with a multimodel ensemble approach using both initialized forecasts (which capture the natural mode part of the prediction) and random initial states (which capture only the forced part of the prediction). They found that the primary part of the skill is dominated by the global warming forcing (Fig. 10a), while the skill due to the natural modes of variability is small and localized in the North Atlantic (Fig. 10b) with very low predictability in the Pacific. However, that study only addressed atmospheric surface variable predictability, while subsurface oceanic predictability associated with Rossby wave propagation can result in enhanced SST forecast skill over interannual timescales (Schneider and Miller 2001; Qiu et al. 2014).

CMIP5 models show the AMOC to weaken under climate change but no models predict a collapse. However, there is some indication that models might be too stable as diagnosed from the cross-equatorial salinity flux. One study with a low-resolution climate model does exhibit bi-stability. A recent study on Abrupt Climate Change by the U.S. Climate Change Science Program concluded that it is very likely that the strength of the AMOC

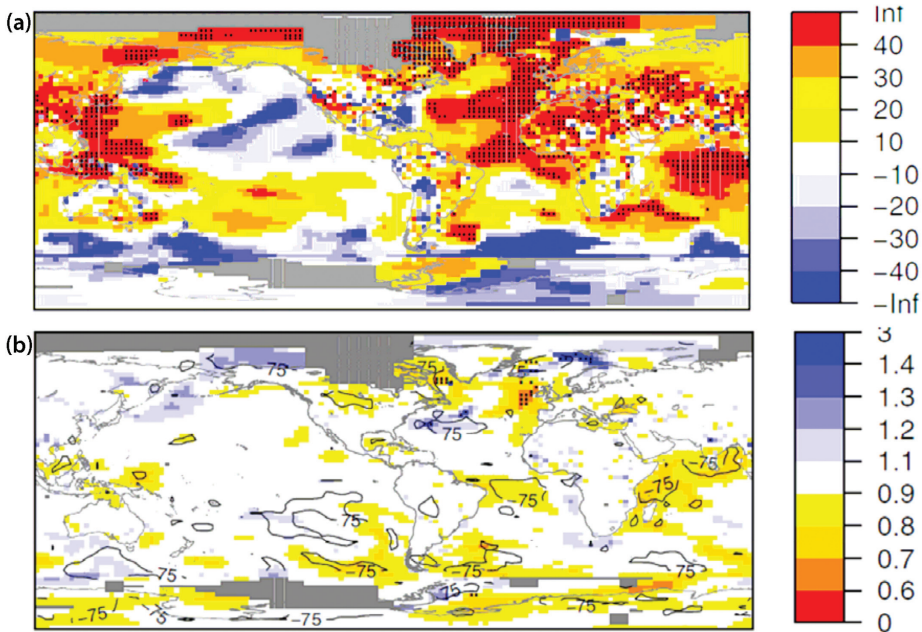


Figure 10. Results from retrospective decadal forecasts from both initialized forecasts (natural-mode part of the prediction) and random initial states (forced part of the prediction) show that the main skill is due to the global-warming forcing. (a) Root mean square skill score (multiplied by 100) of the ensemble mean of the initialized multimodel for predictions averaged over the forecast years 6–9. A combination of observed temperatures over land and over the polar areas is used as a reference. Black dots correspond to the points where the skill score is statistically significant with 95% confidence. (b) Ratio of Root mean square error between the initialized and not-initialized multimodel experiments for predictions averaged over the forecast years 6–9. Contours are used for areas where the ratio of at least 75% of the individual forecast systems has a value above or below 1 in agreement with the multimodel ensemble-mean result. Dots are used for the points where the ratio is statistically significantly above or below 1 with 90% confidence. Poorly observationally sampled areas are masked in gray. From Doblas-Reyes et al. (2013).

will decrease over the 21st century in response to increasing greenhouse gases, with a best estimate decrease of 25%–30% (Delworth et al. 2008). This mainly results from the warming of the North Atlantic on the multidecadal to century timescales, with the aid of the retreat of summer Arctic sea-ice cover in the future 21st century climate projections. Changes in the AMOC and the associated northward flow of warm water could, in turn, affect the reduction of Arctic sea ice and the shrinking of the Greenland Ice Sheet.

Interestingly, the climate change projections for the Mediterranean area obtained from the regional coupled models are generally consistent with the findings obtained with global or regional atmospheric-only models (Gualdi et al. 2013). This agreement suggests that,

in general terms, the regional air–sea coupling does not impact strongly the response to anthropogenic climate change.

In contrast, some RCCMs studies show markedly different climate projections than the global models, due largely to the poorly simulated oceanic dynamical and coastal processes. For example, Seo and Xie (2011), using the SCOAR model, carried out the first RCCM study that regionally downscaled the climate change scenarios based on GFDL climate model. In the equatorial Atlantic, they suggested that the equatorial currents, upwelling, and TIWs strongly control the spatial pattern in SST warming via eddy-driven heat transport, not captured in the GFDL model. This result supports the importance of the ocean dynamical process in regulating regional SST warming patterns under climate change scenarios. Li et al. (2014) also downscaled the NCAR CCSM3 projection of future climate over California to find that near-coast air-temperature warming is significantly reduced in the coupled model compared to that in the atmosphere-only run. The difference is attributed to the lower SST associated with coastal upwelling, not captured in the CCSM. This result further suggests the importance of the ocean dynamical process in regulating regional SST warming patterns and thus the regional climate change patterns.

## 8. Conclusions

We reviewed many aspects of the coupled ocean–atmosphere processes relevant to understanding precipitation impacts, focusing on interannual, decadal, and global-warming timescales. Current GCMs are now capable of capturing many aspects of these key processes and simulate some of the most prominent modes of coupled climate variability. There is a need for regional climate model downscaling and several of the new models have demonstrated impressive abilities in this context. Land-surface processes and frontal-scale air–sea interactions are important crux points for simulations affecting precipitation. Two example regions, the Intra-American Seas and the Mediterranean Basin, show how models and observations can be used together to improve simulations and forecasts. Lastly, we explained many issues related to the theoretical predictability limits of climate problems, the practical limits of making actual predictions, and the expectations for skill associated with global warming projections.

*Acknowledgments.* AJM was supported by the NSF Earth System Modeling Program (OCE1419306) and the NOAA Climate Variability and Prediction Program (NA14OAR4310276). HS thanks the Office of Naval Research for support under N00014-15-1-2588. LPP was supported by “Advanced Studies in Medium and High Latitudes Oceanography” (CAPES 23038.004304/2014-28) and “National Institute of Science and Technology of the Cryosphere” (CNPq/PROANTAR 704222/2009). VM was supported by NOAA grant NA12OAR4310078. TGI was supported by the U. S. Naval Research Laboratory 6.2 project “Fresh Water Balance in the Coupled Ocean-Atmosphere System” (BE-435-040-62435N-6777) YHT was supported by the MOST grant 106-2111-M-002-001, Taiwan.

## REFERENCES

- Alexander, M. A., I. Bladé, M. Newman, J. R. Lanzante, N.-C. Lau and J. D. Scott. 2002. The atmospheric bridge: The influence of ENSO teleconnection on air-sea interaction over the global oceans. *J. Clim.*, *15*, 2205–2231.
- Alfaro, E., A. Gershunov, D. Cayan, A. Steinemann, D. Pierce, and T. Barnett. 2004. A Method for Prediction of California Summer Air Surface Temperature. *EOS, Trans. Am. Geophys. Union*, *85*, 553–558.
- Allard, R., E. Rogers, P. Martin, T. Jensen, P. Chu, T. Campbell and J. Dykes et al. 2014. The US Navy Coupled Ocean-Wave Prediction System. *Oceanography*, *27*, 92–103.
- Alpert, P., M. Baldi, R. Llani, S. Krichak, C. Price, X. Rodo and H. Saaroni et al. 2006. Relation between climate variability in the Mediterranean region and the tropics: ENSO, south Asian and African monsoons, hurricanes and Saharan dust *in* Mediterranean Climate Variability. P. Lionello, P. Malanotte-Rizzoli and R. Boscolo, eds. Amsterdam: Elsevier, 149–177.
- Amaya, D., S.-P. Xie, A. J. Miller and M. J. McPhaden. 2015. Seasonality of tropical Pacific decadal trends during the 21st century global warming hiatus. *J. Geophys. Res. C Oceans*, *120*, 6782–6798.
- Ashok, K., S. Behera, S. Rao, H. Weng and T. Yamagata. 2007. El Niño Modoki and its possible teleconnection. *J. Geophys. Res. C Oceans*, *112*, C11007.
- Baker, N. C. and H. P. Huang. 2014. A comparative study of precipitation and evaporation between CMIP3 and CMIP5 climate model ensembles in semiarid regions. *J. Clim.*, *27*, 3731–3749.
- Barnett, T. P., D. W. Pierce, R. Saravanan, N. Schneider, D. Dommenges and M. Latif. 1999. Origins of the midlatitude Pacific decadal variability. *Geophys. Res. Lett.*, *26*, 1453–56.
- Bellenger, H., E. Guilyardi, J. Leloup, M. Lengaigne and J. Vialard. 2014. ENSO representation in climate models: from CMIP3 to CMIP5. *Clim. Dynam.*, *42*, 1999–2018.
- Bellucci A., S. Gualdi and A. Navarra, 2010. The double-ITCZ syndrome in coupled general circulation models: the role of large-scale vertical circulation regimes *J. Climate*, *23*, 1127–1145.
- Bellucci, A., R. Haarsma, N. Bellouin, B. Booth, C. Cagnazzo, B. van den Hurk and N. Keenlyside et al. 2015. Advancements in decadal climate predictability: The role of nonoceanic drivers. *Rev. Geophys.*, *53*, 165–202.
- Bender, M. A. and I. Ginis. 2000. Real-case simulations of hurricane–ocean interaction using a high-resolution coupled model: effects on hurricane intensity. *Mon. Weather Rev.*, *128*, 917–946.
- Bender, M. A., I. Ginis, R. Tuleya, B. Thomas and T. Marchok. 2007. The operational GFDL coupled hurricane–ocean prediction system and a summary of its performance. *Mon. Weather Rev.*, *135*, 3965–3989.
- Bersch, M., I. Yashayaev and K. Koltermann. 2007. Recent changes of the thermohaline circulation in the subpolar North Atlantic. *Ocean Dynam.*, *57*, 223–235.
- Betts, A. K. and J. H. Ball. 1995. The FIFE surface diurnal cycle climate, *J. Geophys. Res.*, *100(D12)*, 25679–25693.
- Biondi, F., A. Gershunov and D. R. Cayan. 2001. North Pacific decadal climate variability since 1661. *J. Clim.*, *14*, 5–10.
- Boer, G. J. 2011. Decadal potential predictability of twenty-first century climate. *Clim. Dynam.*, *36*, 1119–1133.
- Böning, C. W., M. Scheinert, J. Dengg, A. Biastoch and A. Funk. 2006. Decadal variability of subpolar gyre transport and its reverberation in the North Atlantic overturning. *Geophys. Res. Lett.*, *33*, 5.
- Booij, N., R. C. Ris and L. H. Holthuijsen. 1999. A third-generation wave model for coastal regions 1. Model description and validation. *J. Geophys. Res.*, *104*, 7649–7666.
- National Research Council, Committee on a National Strategy for Advancing Climate Modeling. 2012. A National Strategy for Advancing Climate Modeling. Washington, DC: The National Academies Press, 294 pp.

- Brovkin, V. 2002. Climate-vegetation interaction in ERCA (European Research Course on Atmospheres), vol. 5. C. F. Boutron, ed. Les Ulis, France: EDP Sciences, 57–72.
- Budyko, M. I. 1956. The Heat Balance of the Earth's Surface. Leningrad: Gidrometeoizdat, 255 pp. Russian.
- Budyko, M. I. 1974. Climate and Life. Orlando, Florida: Academic Press, 508 pp.
- Cai, W., S. Borlace, M. Lengaigne, P. van Rensch, M. Collins, G. Vecchi and A. Timmermann et al. 2014. Increasing frequency of extreme El Niño events due to greenhouse warming. *Nat. Clim. Change*, 4, 111–116.
- Cai, W., G. Wang, A. Santoso, M. J. McPhaden, L. Wu, F.-F. Jin and A. Timmermann et al. 2015. Increased frequency of extreme La Niña events under greenhouse warming. *Nat. Clim. Change*, 5, 132–137.
- Capotondi, A., A. T. Wittenberg, M. Newman, E. Di Lorenzo, J. Y. Yu, P. Braconnot and J. Cole et al. 2015. Understanding ENSO diversity. *Bull. Am. Meteorol. Soc.*, 96, 921–938.
- Cattiaux, J., H. Douville, R. Schoetter, S. Parey and P. Yiou. 2015. Projected increase in diurnal and interdiurnal variations of European summer temperatures. *Geophys. Res. Lett.*, 42: 899–907.
- Cayan, D. R. 1992. Latent and sensible heat-flux anomalies over the Northern Oceans—driving the sea surface temperature. *J. Phys. Oceanogr.*, 22, 859–881.
- Chelton, D. B. and S.-P. Xie. 2010. Coupled ocean-atmosphere interaction at oceanic mesoscales. *Oceanography*, 23, 52–69.
- Chen, H. C., C. H. Sui, Y. H. Tseng and B. Huang. 2015. An analysis of the linkage of Pacific Subtropical Cells with the recharge–discharge processes in ENSO evolution. *J. Clim.*, 28, 3786–3805.
- Chen, M., W. Shi, P. Xie, V. B. S. Silva, V. E. Kousky, R. W. Higgins, and J. E. Janowiak. 2008. Assessing objective techniques for gauge-based analyses of global daily precipitation. *J. Geophys. Res.*, 113, D04110.
- Chen, S., M. Flatau, T. G. Jensen, T. Shinoda, J. Schmidt, P. May and J. Cummings et al. 2015. A study of CINDY/DYNAMO MJO suppressed phase. *J. Atmos. Sci.*, 72, 3755–3779.
- Chen, S. S., J. F. Price, W. Zhao, M. A. Donelan and E. J. Walsh. 2007. The CBLAST- Hurricane program and the next-generation fully coupled atmosphere–wave–ocean models for hurricane research and prediction. *Bull. Am. Meteorol. Soc.*, 88, 311–317.
- Chung, C., S. Power, J. Arblaster, H. Rashid and G. Roff. 2014. Nonlinear precipitation response to El Niño and global warming in the Indo-Pacific. *Clim. Dynam.*, 42, 1837–1856.
- Clark, P. U., N. G. Pisias, T. F. Stocker and A. J. Weaver. 2002. The role of the thermohaline circulation in abrupt climate change. *Nature*, 415, 863–869.
- Clement, A. C., R. Seager and R. Murtugudde. 2001. Why are there tropical warm pools? *J. Clim.*, 18, 5294–5311.
- Collins, M., S.-I. An, W. Cai, A. Ganachaud, E. Guilyardi, F.-F. Jin and M. Jochum et al. 2010. The impact of global warming on the tropical Pacific Ocean and El Niño. *Nat. Geosci.*, 3, 391–397.
- Compo, G., J. Whitaker, P. Sardeshmukh, N. Matsui, R. Allan, X. Yin and B. Gleason et al. 2011. The Twentieth Century Reanalysis Project. *Q. J. Roy. Meteorol. Soc.*, 137, 1–28.
- Cook, K. H. and E. K. Vizy. 2006. Coupled model simulations of the West African monsoon system: Twentieth-and twenty-first-century simulations. *J. Clim.* 19, 3681–3703.
- Danabasoglu, G., S. G. Yeager, Y.-O. Kwon, J. J. Tribbia, A. S. Phillips and J. W. Hurrell. 2012. Variability of the Atlantic meridional overturning circulation in CCSM4. *J. Clim.*, 25, 5153–5172.
- D'Arrigo, R., R. Villalba and G. Wiles. 2001. Tree-ring estimates of Pacific decadal climate variability. *Clim. Dynam.*, 18, 219–224.

- Dee, D., S. Uppala, A. Simmons, P. Berrisford, P. Poli, S. Kobayashi and U. Andrae et al. 2011. The ERA-Interim reanalysis: configuration and performance of the data assimilation system. *Q. J. Roy. Meteorol. Soc.*, *137*, 553–597.
- DeFlorio, M. J., D. W. Pierce, D. R. Cayan and A. J. Miller. 2013. Western U.S. extreme precipitation events and their relation to ENSO and PDO in CCSM4. *J. Clim.*, *26*, 4231–4243.
- Delworth, T. L., P. U. Clark, M. Holland, W. E. Johns, T. Kuhlbrodt, J. Lynch-Stieglitz and C. Morrill et al. 2008. The potential for abrupt change in the Atlantic Meridional Overturning Circulation *in* Abrupt Climate Change. A Report by the U.S. Climate Change Science Program and the Subcommittee on Global Change Research. Reston, Virginia: U. S. Geological Survey, 258–359.
- Delworth, T. L. and R. J. Greatbatch. 2000. Multidecadal thermohaline circulation variability driven by atmospheric surface flux forcing. *J. Clim.*, *13*, 1481–1495.
- Delworth, T. L., S. Manabe and R. J. Stouffer. 1993. Interdecadal variations of the thermohaline circulation in a coupled ocean-atmosphere model. *J. Clim.*, *6*, 1993–2011.
- Deser, C., A. S. Phillips and J. W. Hurrell. 2004. Pacific interdecadal climate variability: Linkages between the tropics and the North Pacific during the boreal winter since 1900. *J. Clim.*, *17*, 3109–3124.
- Deser, C., A. S. Phillips, R. A. Tomas, Y. M. Okumura, M. A. Alexander, A. Capotondi and J. D. Scott et al. 2011. ENSO and Pacific Decadal Variability in Community Climate System Model Version 4. *J. Clim.*, *25*, 2622–2651.
- Deshayes, J. and C. Frankignoul. 2008. Simulated variability of the circulation in the North Atlantic from 1953 to 2003. *J. Clim.*, *21*, 4919–4933.
- Dickson, R. R., J. Lazier, J. Meincke, P. Rhines and J. Swift. 1996. Long-term coordinated changes in the convective activity of the North Atlantic. *Progr. Oceanogr.*, *38*, 241–295.
- Diffenbaugh, N. S. and F. Giorgi. 2012. Climate change hotspots in the CMIP5 global climate model ensemble. *Climatic Change*, *114*, 813–822.
- Di Lorenzo, E., K. M. Cobb, J. C. Furtado, N. Schneider, B. T. Anderson, A. Bracco and M. A. Alexander et al. 2010. Central Pacific El Niño and decadal climate change in the North Pacific Ocean. *Nat. Geosci.*, *3*, 762–765.
- Di Lorenzo, E., N. Schneider, K. M. Cobb, P. J. S. Franks, K. Chhak, A. J. Miller and J. C. McWilliams et al. 2008. North Pacific Gyre Oscillation links ocean climate and ecosystem change. *Geophys. Res. Lett.*, *35*, L08607.
- Doblas-Reyes F. J., I. Andreu-Burillo, Y. Chikamoto, J. García-Serrano, V. Guemas, M. Kimoto and T. Mochizuki et al. 2013. Initialized near-term regional climate change prediction. *Nat. Comm.*, *4*, 1715.
- Doherty, R., J. E. Kutzbach, J. A. Foley and D. Pollard. 2000. Fully coupled climate/dynamical vegetation model simulations over northern Africa during the mid-Holocene. *Clim. Dynam.*, *16*, 561–573.
- Douville, H. 2010. Relative contribution of soil moisture and snow mass to seasonal climate predictability: a pilot study. *Clim. Dynam.*, *34*, 797–818.
- Douville, H., D. Salas-Méllia and S. Tyteca. 2006. On the tropical origin of uncertainties in the global land precipitation response to global warming. *Clim. Dynam.*, *26*, 367–385.
- Dubois, C., S. Somot, S. Calmanti, A. Carillo, M. Déqué, A. Dell’Aquila and A. Elizalde et al. 2012. Future projections of the surface heat and water budgets of the Mediterranean Sea in an ensemble of coupled atmosphere-ocean regional climate models. *Clim. Dynam.*, *39*, 1859–1884.
- ESGF-CoG (Earth System Grid Federation-CoG). 2017. “Community Infrastructure for Building and Coupling Models.” Earth System Modeling Framework, Version 7.0.1. Last modified March 3, 2017. <https://www.earthsystemcog.org/projects/esmf/>

- Eden, C. and R. J. Greatbatch. 2003. A damped decadal oscillation in the North Atlantic climate system. *J. Clim.*, *16*, 4043–4060.
- Eden, C. and T. Jung. 2001. North Atlantic interdecadal variability: Oceanic response to the North Atlantic oscillation (1865–1997). *J. Clim.*, *14*, 676–691.
- Eden, C. and J. Willebrand. 2001. Mechanism of interannual to decadal variability of the North Atlantic circulation. *J. Clim.*, *14*, 2266–2280.
- Eden, C. and H. Dietze. 2009. Effects of mesoscale eddy/wind interactions on biological new production and eddy kinetic energy. *J. Geophys. Res.*, *114*, C05023.
- Elguindi, N., S. Somot, M. Déqué and W. Ludwig. 2009. Climate change evolution of the hydrological balance of the Mediterranean, Black and Caspian Seas: impact of climate model resolution. *Clim. Dynam.*, *36*, 205–228.
- Eltahir, E. A. B. 1998. A soil moisture–rainfall feedback mechanism: 1. Theory and observations. *Water Resour. Res.*, *34*, 765–776.
- England, M., S. McGregor, P. Spence, G. Meehl, A. Timmermann, W. Cai and A. Sen Gupta et al. 2014. Recent intensification of wind-driven circulation in the Pacific and the ongoing warming hiatus. *Nat. Clim. Change*, *4*, 222–227.
- Esselborn, S. and C. Eden. 2001. Sea surface height changes in the North Atlantic Ocean related to the North Atlantic Oscillation. *Geophys. Res. Lett.*, *28*, 3473–3476. doi: 10.1029/2001GL012863
- ENES (European Network for Earth System modelling). 2011. The OASIS coupler. <https://verc.enes.org/oasis/>
- Farneti, R., F. Molteni and F. Kucharski. 2014. Pacific interdecadal variability driven by tropical–extratropical interactions. *Clim. Dynam.*, *42*, 3337–3355.
- Fennessy, M. J. and J. Shukla. 1999. Impact of initial soil wetness on seasonal atmospheric prediction. *J. Clim.*, *12*, 3167–3180.
- Ferranti, L. and P. Viterbo. 2006. The European summer of 2003: Sensitivity to soil water initial conditions. *J. Clim.*, *19*, 3659–3680.
- Fischer, E. M. and C. Schär. 2009. Future changes in daily summer temperature variability: driving processes and role for temperature extremes. *Clim. Dynam.*, *33*, 917–935.
- Flaounas, E., P. Drobinski, M. Vrac, S. Bastin, C. Lebeaupin-Brossier, M. Stéfanon, M. Borga, and J.-C. Calvet. 2013. Precipitation and temperature space-time variability and extremes in the Mediterranean region: evaluation of dynamical and statistical downscaling methods. *Clim. Dynam.*, *40*, 2687–2705.
- Frankignoul, C. and K. Hasselmann. 1977. Stochastic climate models. Part II. Application to SST anomalies and thermocline variability. *Tellus*, *29*, 289–305.
- Frierson, D. M. W., Y.-T. Hwang, N. S. Fuckar, R. Seager, S. M. Kang, A. Donohoe and E. A. Maroon et al. 2013. Contribution of ocean overturning circulation to tropical rainfall peak in the Northern Hemisphere. *Nat. Geosci.*, *6*, 940–944.
- Furtado, J. C., E. Di Lorenzo, N. Schneider and N. A. Bond. 2011. North Pacific decadal variability and climate change in the IPCC AR4 models. *J. Clim.*, *24*, 3049–3067.
- Gedalof, Z. and D. J. Smith. 2001. Interdecadal climate variability and regime-scale shifts in Pacific North America. *Geophys. Res. Lett.*, *28*, 1515–1518.
- Gent, P. R., G. Danabasoglu, L. J. Donner, M. M. Holland, E. C. Hunke, S. R. Jayne and D. M. Lawrence et al. 2011. The Community Climate Model Version 4. *J. Clim.*, *24*, 4973–4991.
- Gent, P., S. Yeager, R. B. Neale, S. Levis and D. Bailey. 2010. Improvements in a half degree atmosphere/land version of the CCSM. *Clim. Dynam.*, *34*, 819–833.
- Gershunov, A. and T. P. Barnett. 1998. Interdecadal modulation of ENSO teleconnections. *Bull. Am. Meteorol. Soc.*, *79*, 2715–2725.
- Giorgi, F. 2006. Climate change hot-spots. *Geophys. Res. Lett.*, *33*, L08707.

- Gualdi, S., S. Somot, L. Li, V. Artale, M. Adani, A. Bellucci and A. Braun et al. 2013. The CIRCE simulations: Regional climate change projections with realistic representation of the Mediterranean Sea. *Bull. Am. Meteorol. Soc.*, *94*, 65–81.
- Gustafsson, N., L. Nyberg, and A. Omstedt, 1998. Coupling of a high-resolution atmospheric model and an ocean model for the Baltic Sea. *Mon. Wea. Rev.*, *126*, 2822–2846.
- Haidvogel, D. B., H. Arango, W. P. Budgell, B. D. Cornuelle, E. Curchitser, E. Di Lorenzo and K. Fennel et al. 2008. Ocean forecasting in terrain-following coordinates: Formulation and skill assessment of the Regional Ocean Modeling System. *J. Comput. Phys.*, *227*, 3595–3624.
- Häkkinen, S. 2001. Variability in sea surface height: A qualitative measure for the meridional overturning in the North Atlantic. *J. Geophys. Res.*, *106*, 13837–13848.
- Häkkinen, S. and P. B. Rhines. 2004. Decline of subpolar North Atlantic circulation during the 1990s. *Science*, *304*, 555–559.
- Hall, I. R., S. B. Moran, R. Zahn, P. C. Knutz, C. C. Shen and R. L. Edwards. 2006. Accelerated drawdown of meridional overturning in the late-glacial Atlantic triggered by transient pre-H event freshwater perturbation. *Geophys. Res. Lett.*, *33*. doi: 10.1029/2006gl026239
- Hare, S. R. and N. J. Mantua. 2000. Empirical evidence for North Pacific regime shifts in 1977 and 1989. *Progr. Oceanogr.*, *47*, 103–145.
- Hasselmann, K. 1976. Stochastic climate models. Part I. Theory. *Tellus*, *28*, 473–485.
- Hawkins, E., R. S. Smith, L. C. Allison, J. M. Gregory, T. J. Woollings, H. Pohlmann and B. de Cuevas. 2011. Bistability of the Atlantic overturning circulation in a GCM and links to ocean freshwater transport. *Geophys. Res. Lett.*, *38*, L10605.
- Held, I. and B. Soden. 2006. Robust responses of the hydrological cycle to global warming. *J. Clim.*, *19*, 5686–5699.
- Hendon, H. H., M. Wheeler and C. Zhang. 2007. Seasonal dependence of the MJO-ENSO relationship. *J. Clim.*, *20*, 531–543.
- Higgins, W. and W. Shi. 2001. Intercomparison of the principal modes of interannual and intraseasonal variability of the North American monsoon system. *J. Clim.*, *14*, 403–417.
- Hillaire-Marcel, C., A. de Vernal, G. Bilodeau and A. J. Weaver. 2001. Absence of deep-water formation in the Labrador Sea during the last interglacial period. *Nature*, *410*, 1073–1077.
- Hu, Z.-Z., A. Kumar, H.-L. Ren, H. Wang, M. L'Heureux and F.-F. Jin. 2013. Weakened interannual variability in the tropical Pacific Ocean since 2000. *J. Clim.*, *26*, 2601–2613.
- Hurrell, J. W., Y. Kushnir, G. Ottersen and M. Visbeck. 2003. An overview of the North Atlantic Oscillation in *The North Atlantic Oscillation: Climatic Significance and Environmental Impact*, J. W. Hurrell, Y. Kushnir, G. Ottersen and M. Visbeck, eds. Washington, D. C.: American Geophysical Union. doi: 10.1029/134GM01
- Hurrell, J. W., M. Visbeck, A. Busalacchi, R. A. Clarke, T. L. Delworth, R. R. Dickson and W. E. Johns et al. 2006. Atlantic climate variability and predictability: A CLIVAR perspective. *J. Clim.*, *19*, 5100–5121.
- Hwang, Y.-T. and D. M. W. Frierson. 2013. Link between the double intertropical convergence zone problem and cloud biases over the Southern Ocean. *Proc. Nat. Acad. Sci.*, *110*, 4935–4940.
- IPCC. 2007. *Climate Change 2007: The Physical Science Basis*. Contribution of Working Group I to the Fourth Assessment Report of the Intergovernmental Panel on Climate Change. S. Solomon, D. Qin, M. Manning, Z. Chen, M. Marquis, K. B. Averyt, M. Tignor and H. L. Miller, eds. Cambridge, United Kingdom and New York, NY, USA: Cambridge University Press.
- IPCC. 2013. *Climate Change 2013: The Physical Science Basis*. Contribution of Working Group I to the Fifth Assessment Report of the Intergovernmental Panel on Climate Change T. F. Stocker, D. Qin, G.-K. Plattner, M. Tignor, S. K. Allen, J. Boschung, A. Nauels, Y. Xia, V. Bex and P. M.

- Midgley, eds. Cambridge, United Kingdom and New York, NY, USA: Cambridge University Press, 1535 pp.
- Jensen, T. G., T. J. Campbell, R. A. Allard, R. J. Small and T. Smith. 2011. Turbulent heat fluxes during an intense cold-air outbreak over the Kuroshio Extension Region: Results from a high-resolution coupled atmosphere-ocean model. *Ocean Dynam.*, *61*, 657–674.
- Jensen, T. G., T. Shinoda, S. Chen and M. Flatau. 2015. Ocean response to CINDY/DYNAMO MJOs in air-sea coupled COAMPS. *J. Meteorol. Soc. Japan*, *93A*, 157–178.
- Jensen, T. G., H. W. Wijesekera, E. S. Nyadjro, P. Thoppil, J. F. Shriver, K. K. Sandeep, and V. Pant. 2016. Modeling salinity exchanges between the equatorial Indian Ocean and the Bay of Bengal. *Oceanography*, *29*, 92–101.
- Jin, D., D. E. Waliser and C. Jones. 2012. Modulation of tropical ocean surface chlorophyll by the Madden-Julian Oscillation. *Clim. Dynam.*, *40*, 39–58.
- Jochum, M. 2009. Impact of latitudinal variations in vertical diffusivity on climate simulations. *J. Geophys. Res.*, *114(C1)*, C01010.
- Jochum, M. and J. Potemra. 2008. Sensitivity of tropical rainfall to Banda Sea diffusivity in the Community Climate System Model. *J. Clim.*, *21*, 6445–6454.
- Mantua, N. 2017. “PDO index monthly values: January 1900–present.” The Pacific Decadal Oscillation (PDO). Seattle: University of Washington. <http://research.jisao.washington.edu/pdo/PDO.latest.txt>
- Jones, C. 2000. The influence of intraseasonal variations on medium-to extended-range weather forecasts over South America. *Mon. Weather Rev.*, *128*, 486–494.
- Juang, H.-M. H., S.-Y. Hong and M. Kanamitsu. 1997. The NCEP regional spectral model: An update. *Bull. Am. Meteorol. Soc.*, *78*, 2125–2143.
- Kay, J. E., B. R. Hillman, S. A. Klein, Y. Zhang, B. Medeiros, R. Pincus and A. Gettelman et al. 2012. Exposing global cloud biases in the Community Atmosphere Model (CAM) using satellite observations and their corresponding instrument simulators. *J. Clim.*, *25*, 5190–5207.
- Kelley, C., M. Ting, R. Seager and Y. Kushnir. 2012. Mediterranean precipitation climatology, seasonal cycle, and trend as simulated by CMIP5. *Geophys. Res. Lett.*, *39*, L21703.
- Kim, H.-M., P. J. Webster and J. A. Curry. 2012. Evaluation of short-term climate change prediction in multi-model CMIP5 decadal hindcasts. *Geophys. Res. Lett.*, *39*, L10701.
- Kosaka, Y. and S. Xie. 2013. Recent global-warming hiatus tied to equatorial Pacific surface cooling. *Nature*, *501*, 403–407.
- Koster, R. D., P. A. Dirmeyer, Z. Guo, G. Bonan, E. Chan, P. Cox and C. T. Gordon et al. 2004. Regions of strong coupling between soil moisture and precipitation. *Science*, *305*, 1138–1140.
- Kozar, M. and V. Misra. 2012. Evaluation of twentieth-century Atlantic warm pool simulations in historical CMIP5 runs. *Clim. Dynam.*, *41*, 2375–2391.
- Kumar, A., H. Wang, W. Wang, Y. Xue and Z.-Z. Hu. 2013. Does knowing the oceanic PDO phase help predict the atmospheric anomalies in subsequent months? *J. Clim.*, *26*, 1268–1285.
- Lab Sea Group. 1998. The Labrador Sea deep convection experiment. *Bull. Am. Meteorol. Soc.*, *79*, 2033–2058.
- Large, W. G., G. Danabasoglu, J. C. McWilliams, P. R. Gent and F. O. Bryan. 2001. Equatorial circulation of a global ocean climate model with anisotropic horizontal viscosity. *J. Phys. Oceanogr.*, *31*, 518–536.
- Latif, M., M. Collins, H. Pohlmann and N. Keenlyside. 2006. A review of predictability studies of the Atlantic sector climate on decadal time scales. *J. Clim.*, *19*, 5971–5987.
- Lee S.-K., C. Wang and B. E. Mapes. 2009. A simple atmospheric model of the local and teleconnection responses to tropical heating anomalies. *J. Clim.*, *22*, 227–284.

- Lee, T. and M. McPhaden. 2010. Increasing intensity of El Niño in the central-equatorial Pacific. *Geophys. Res. Lett.*, *37*, L14603.
- Lesser, G. R., J. A. Roelvink, T. M. van Kester and G. S. Stelling. 2004. Development and validation of a three-dimensional morphological model. *Coast. Eng.*, *51*, 883–915.
- Li, H. Q., M. Kanamitsu, S. Y. Hong, K. Yoshimura, D. R. Cayan and V. Misra. 2014. A high-resolution ocean–atmosphere coupled downscaling of the present climate over California. *Clim. Dynam.*, *42*, 701–714.
- Lienert, F., J. C. Fyfe and W. J. Merryfield. 2011. Do climate models capture the tropical influences on North Pacific sea surface temperature variability? *J. Clim.*, *24*, 6203–6209.
- Lin, J. L. 2007. The double-ITCZ problem in IPCC AR4 coupled GCMs: Ocean–atmosphere feedback analysis. *J. Clim.*, *20*, 4497–4525.
- Liu, H., C. Wang, S.-K. Lee and D. B. Enfield. 2012. Atlantic warm pool variability in the IPCC AR4 CGCM simulations. *J. Clim.*, *25*, 5612–5628.
- Liu, H., C. Wang, S.-K. Lee and D. B. Enfield. 2013. Atlantic warm pool variability in the CMIP5 simulations. *J. Clim.*, *26*, 5315–5336.
- Livneh, B., E. A. Rosenberg, C. Lin, B. Nijssen, V. Mishra, K. M. Andreadis and E. P. Maurer et al. 2014. A long-term hydrologically based dataset of land surface fluxes and states for the conterminous United States: Update and extensions. *J. Clim.*, *26*, 477–486.
- Lohmann, K., H. Drange and M. Bentsen. 2009. A possible mechanism for the strong weakening of the North Atlantic subpolar gyre in the mid-1990s. *Geophys. Res. Lett.*, *36*, L15602.
- Lorbacher, K., J. Dengg, C. W. Boning and A. Biastoch. 2010. Regional patterns of sea level change related to interannual variability and multidecadal trends in the Atlantic meridional overturning circulation. *J. Clim.*, *23*, 4243–4254.
- Lynch-Stieglitz, J., J. F. Adkins, W. B. Curry, T. Dokken, I. R. Hall, J. C. Herguera and J. J.-M. Hirschi et al. 2007. Atlantic meridional overturning circulation during the Last Glacial Maximum. *Science*, *316*, 66–69.
- Lynch-Stieglitz, J., M. W. Schmidt and W. B. Curry. 2011. Evidence from the Florida Straits for Younger Dryas ocean circulation changes. *Paleoceanography*, *26*, PA1205.
- Ma, X., Z. Jing, P. Chang, X. Liu, R. Montuoro, R. J. Small and F. O. Bryan et al. 2016. Western boundary currents regulated by interaction between ocean eddies and the atmosphere. *Nature*, *535*, 533–537.
- MacDonald, G. M. and R. A. Case. 2005. Variations in the Pacific Decadal Oscillation over the past millennium. *Geophys. Res. Lett.*, *32*, L08703.
- Maes, C., G. Madec and P. Delecluse. 1997. Sensitivity of an equatorial Pacific OGCM to the Lateral Diffusion. *Mon. Weather Rev.*, *125*, 958–971.
- Maloney, E. D. and D. L. Harmann. 2000. Modulation of hurricane activity in the Gulf of Mexico by the Madden-Julian Oscillation. *Science*, *287*, 2002–2004.
- Mantua, N., S. Hare, Y. Zhang, J. Wallace and R. Francis. 1997. A Pacific interdecadal climate oscillation with impacts on salmon production. *Bull. Am. Meteorol. Soc.*, *78*, 1069–1079.
- Marcos, M. and M. N. Tsimplis. 2008. Comparison of results of AOGCMs in the Mediterranean Sea during the 21st century. *J. Geophys. Res.*, *113*, C12028.
- Mariotti, A. and A. Dell’Aquila. 2012. Decadal climate variability in the Mediterranean region: roles of large-scale forcings and regional processes. *Clim Dynam.*, *38*, 1129–1145.
- Mariotti, A., N. Zeng and K.-M. Lau. 2002. Euro-Mediterranean rainfall and ENSO—A seasonally varying relationship. *Geophys. Res. Lett.*, *29*, 1621.
- Marshall, A., O. Alves and H. H. Hendon. 2009. A coupled GCM analysis of MJO activity at the onset of El Niño. *J. Atmos. Sci.*, *66*, 966–983.

- Materia, S., A. Borrelli, A. Bellucci, A. Alessandri, P. Di Pietro, P. Athanasiadis and A. Navarra et al. 2014. Impact of atmosphere and land surface initial conditions on seasonal forecast of global surface temperature. *J. Clim.*, *29*, 9253–9271.
- McGowan, J. A., S. J. Bograd, R. J. Lynn and A. J. Miller. 2003. The biological response to the 1977 regime shift in the California Current. *Deep Sea Res.*, *50*, 2567–2582.
- McManus, J. F., R. Francois, J. M. Gherardi, L. D. Keigwin and S. Brown-Leger. 2004. Collapse and rapid resumption of Atlantic meridional circulation linked to deglacial climate changes. *Nature*, *428*, 834–837.
- McPhaden, M. J., T. Lee and D. McClurg. 2011. El Niño and its relationship to changing background conditions in the tropical Pacific. *Geophys. Res. Lett.* *38*, L15709.
- Mechoso, C. R., A. W. Robertson, N. Barth, M. K. Davey, P. Delecluse, P. R. Gent and S. Ineson et al. 1995. The seasonal cycle over the tropical Pacific in coupled ocean–atmosphere general circulation models. *Mon. Weather. Rev.*, *123*, 2825–2838.
- Meehl, G. A., A. Hu, J. M. Arblaster, J. Fasullo and K. E. Trenberth. 2013. Externally forced and internally generated decadal climate variability associated with the Interdecadal Pacific Oscillation. *J. Clim.*, *26*, 7298–7310.
- Meehl, G. A. and H. Teng. 2012. Case studies for initialized decadal hindcasts and predictions for the Pacific region. *Geophys. Res. Lett.*, *39*, L22705.
- Miller, A. J., F. Chai, S. Chiba, J. R. Moisan and D. J. Neilson. 2004. Decadal-scale climate and ecosystem interactions in the North Pacific Ocean. *J. Oceanogr.*, *60*, 163–188.
- Miller, A. J. and N. Schneider. 2000. Interdecadal climate regime dynamics in the North Pacific Ocean: Theories, observations and ecosystem impacts. *Progr. Oceanogr.*, *47*, 355–379.
- Minobe, S., A. Kuwano-Yoshida, N. Komori, S.-P. Xie and R. Small. 2008. Influence of the Gulf Stream on the troposphere. *Nature*, *452*, 206–209.
- Miralles, D. G., M. J. vanden Berg, A. J. Teuling and R. A. M. deJeu. 2012. Soil moisture-temperature coupling: A multiscale observational analysis. *Geophys. Res. Lett.*, *39*, L21707.
- Misra, V., S. Chan, R. Wu and E. Chassignet. 2009. Air-sea interaction over the Atlantic warm pool in the NCEP CFS. *Geophys. Res. Lett.*, *36*, L15702.
- Misra, V. and S. DiNapoli. 2013. Understanding wet season variations over Florida. *Clim. Dynam.*, *40*, 1361–1372.
- Misra, V., H. Li and M. Kozar. 2014. The precursors in the Intra-American Seas to boreal summer and fall seasonal climate variations over the United States and Mesoamerica. *J. Geophys. Res. C Oceans*, *119*, 2938–2948.
- Misra, V., L. Moeller, L. Stefanova, S. Chan, J. J. O'Brien, T. J. Smith III and N. Plant. 2011. The influence of Atlantic Warm Pool on Panhandle Florida Sea Breeze. *J. Geophys. Res.*, *116*, D00Q06.
- Misra, V., A. Stroman and S. DiNapoli. 2013. The rendition of the Atlantic warm pool in the reanalyses. *Clim. Dynam.* *41*, 517.
- Moon, J., B. Wang and K.-J. Ha. 2011. ENSO regulation of MJO teleconnection. *Clim. Dynam.*, *37*, 1133–1149.
- Navarra, A. I. and L. Tubiana, eds. 2013. *Regional Assessment of Climate Change in the Mediterranean*. Volume 1: Air, Sea and Precipitation and Water. Dordrecht, New York: Springer, 338 pp.
- Neale, R. B., J. Richter and M. Jochum. 2008. The impact of convection on ENSO: From a delayed oscillator to a series of events. *J. Clim.*, *21*, 5904–5924.
- Neale, R. B., J. Richter, S. Park, P. H. Lauritzen, S. J. Vavrus, P. J. Rasch and M. Zhang. 2013. The mean climate of the Community Atmosphere Model (CAM4). *J. Clim.*, *26*, 5150–5168.
- Newman, M., M. A. Alexander, T. R. Ault, K. M. Cobb, C. Deser, E. Di Lorenzo and N. J. Mantua et al. 2016. The Pacific decadal oscillation, revisited. *J. Clim.*, *29*, 4399–4427.

- Newman, M., G. P. Compo and M. A. Alexander. 2003. ENSO-forced variability of the Pacific Decadal Oscillation. *J. Clim.*, *16*, 3853–3857.
- O'Neill, L. W., D. B. Chelton and S. K. Esbensen. 2012. Covariability of surface wind and stress response to sea surface temperature fronts. *J. Clim.*, *25*, 5916–5942.
- Palmer, T. 2014. Build high-resolution global climate models. *Nature*, *515*, 338–339.
- Paolino, D., J. L. Kinter, B. P. Kirtman, D. Min and D. M. Straus. 2012. The impact of land surface and atmospheric initialization on seasonal forecasts with CCSM. *J. Clim.*, *25*, 1007–1021.
- Pezzi, L. P. 2003. Equatorial Pacific Dynamics: Lateral Mixing and Tropical Instability Waves. Ph.D. diss., School of Ocean and Earth Sciences, University of Southampton, United Kingdom. 126 pp.
- Pezzi, L. P. and I. F. A. Cavalcanti. 2001. The relative importance of ENSO and tropical Atlantic sea surface temperature anomalies for seasonal precipitation over South America: A numerical study. *Clim. Dynam.*, *17*, 205–212.
- Pezzi, L. P. and K. J. Richards. 2003. Effects of lateral mixing on the mean state and eddy activity of an equatorial ocean. *J. Geophys. Res.*, *108*, 3371.
- Pezzi, L. P., R. B. Souza, M. S. Dourado, C. A. E. Garcia, M. M. Mata and M. A. F. Silva-Dias. 2005. Ocean-atmosphere in situ observations at the Brazil-Malvinas Confluence region, *Geophys. Res. Lett.*, *32*, L22603.
- Pezzi, L. P., J. Vialard, K. J. Richards, C. Menkes and D. Anderson. 2004. Influence of ocean atmosphere coupling on the properties of tropical instability waves. *Geophys. Res. Lett.*, *31*, L16306.
- Philander, S. G. 1990. *El Niño, La Niña, and the Southern Oscillation*. San Diego: Academic Press, 283 pp.
- Pierce, D. W. 2001. Distinguishing coupled ocean-atmosphere interactions from background noise in the North Pacific. *Progr. Oceanogr.*, *49*, 331–352.
- Pierce, D. W. 2002. The role of sea surface temperatures in interactions between ENSO and the North Pacific Oscillation. *J. Clim.*, *15*, 1295–1308.
- Pitman, A. J. 2003. The evolution of, and revolution in, land surface schemes designed for climate models. *Int. J. Climatol.*, *23*, 479–510.
- Power, S., T. Casey, C. Folland, A. Colman and V. Mehta. 1999. Interdecadal modulation of the impact of ENSO on Australia. *Clim. Dynam.*, *15*, 319–324.
- Power, S., F. Delage, C. Chung, G. Kociuba and K. Keay. 2013. Robust twenty-first-century projections of El Niño and related precipitation variability. *Nature*, *502*, 541–545.
- Putrasahan, D. A., A. J. Miller and H. Seo. 2013a. Isolating mesoscale coupled ocean-atmosphere interactions in the Kuroshio Extension region. *Dynam. Atmos. Oceans*, *63*, 60–78.
- Putrasahan, D. A., A. J. Miller and H. Seo. 2013b. Regional coupled ocean-atmosphere downscaling in the Southeast Pacific: impacts on upwelling, mesoscale air-sea fluxes, and ocean eddies. *Ocean Dynam.*, *63*, 463–488.
- Qiu, B., S. Chen, N. Schneider and B. Taguchi. 2014. A coupled decadal prediction of the dynamic state of the Kuroshio Extension system. *J. Clim.*, *27*, 1751–1764.
- Renault, L., M. J. Molemaker, J. C. McWilliams, A. F. Shchepetkin, F. Lemarié, D. Chelton, S. Illig, and A. Hall, 2016. Modulation of wind work by oceanic current interaction with the atmosphere. *J. Phys. Oceanogr.*, *46*, 1685–1704.
- Rhein, M., D. Kieke, S. Huttel-Kabus, A. Roessler, C. Mertens, R. Meissner and B. Klein et al. 2011. Deep water formation, the subpolar gyre, and the Meridional Overturning Circulation in the subpolar North Atlantic. *Deep Sea Res. II*, *58*, 1819–1832.
- Rind, D., P. deMenocal, G. Russell, S. Sheth, D. Collins, G. Schmidt and J. Teller. 2001. Effects of glacial meltwater in the GISS coupled atmosphere-ocean model 1. North Atlantic Deep Water response. *J. Geophys. Res.*, *16*, 27335–27353.

- Roberts, C.D., M. D. Palmer, D. McNeall and M. Collins. 2015. Quantifying the likelihood of a continued hiatus in global warming. *Nat. Clim. Change*, *5*, 337–342.
- Rodwell, M. J. and B. J. Hoskins. 1996. Monsoons and the dynamic of deserts. *Q. J. Roy. Meteorol. Soc.*, *122*, 1385–1404.
- Roehrig, R., D. Bouniol, F. Guichard, F. Hourdin and J. L. Redelsperger. 2013. The present and future of the West African monsoon: A process-oriented assessment of CMIP5 simulations along the AMMA transect. *J. Clim.*, *26*, 1–88.
- Saha, S., S. Moorthi, H.-L. Pan, X. Wu, J. Wang, S. Nadiga and P. Tripp et al. 2010. The NCEP Climate Forecast System Reanalysis. *Bull. Am. Meteorol. Soc.*, *91*, 1015–1057.
- Sanna A., P. Lionello and S. Gualdi. 2013. Coupled atmosphere ocean climate model simulations in the Mediterranean region: Effect of a high-resolution marine model on cyclones and precipitation. *Nat. Hazards Earth Syst. Sci.*, *13*, 1567–1577.
- Sardeshmukh, P. and P. Sura. 2007. Multiscale impacts of variable heating in climate. *J. Clim.*, *20*, 5677–5695.
- Schär, C., D. Lüthi, U. Beyerle and E. Heise. 1999. The soil-precipitation feedback: A process study with a regional climate model. *J. Clim.*, *12*, 722–741.
- Schneider, N. and B. D. Cornuelle. 2005. The forcing of the Pacific decadal oscillation. *J. Clim.*, *18*, 4355–4373.
- Schneider, N. and A. J. Miller. 2001. Predicting western North Pacific Ocean climate. *J. Clim.*, *14*, 3997–4002.
- Schneider, N., A. J. Miller and D. W. Pierce. 2002. Anatomy of North Pacific decadal variability. *J. Clim.*, *15*, 586–605.
- Sellers, P. J., L. Bounoua, G. J. Collatz, D. A. Randall, D. A. Dazlich, S. O. Los and J. A. Berry et al. 1996. Comparison of radiative and physiological effects of doubled atmospheric CO<sub>2</sub> on climate. *Science*, *271*, 1402–1406.
- Sellers, P. J., R. E. Dickinson, D. A. Randall, A. K. Betts, F. G. Hall, J. A. Berry, G. J. Collatz, A. S. Denning, H. A. Mooney, C. A. Nobre, N. Sato, C. B. Field and A. Henderson-Sellers. 1997. Modeling the exchanges of energy, water, and carbon between continents and the atmosphere. *Science*, *275*, 502–509.
- Seneviratne, S. I., T. Corti, E. L. Davin, M. Hirschi, E. B. Jaeger, I. Lehner and B. Orlowsky et al. 2010. Investigating soil moisture–climate interactions in a changing climate: A review, *Earth Sci. Rev.*, *99*, 125–161.
- Seneviratne, S. I., D. Lüthi, M. Litschi and C. Schär. 2006. Land–atmosphere coupling and climate change in Europe. *Nature*, *443*, 205–209.
- Seo, H., M. Jochum, R. Murtugudde, A. J. Miller and J. O. Roads. 2007. Feedback of tropical instability wave-induced atmospheric variability onto the ocean. *J. Clim.*, *20*, 5842–5855.
- Seo, H., A. J. Miller and J. R. Norris. 2016. Eddy-wind interaction in the California Current System: Dynamics and impacts. *J. Phys. Oceanogr.*, *46*, 439–459.
- Seo, H., A. Miller and J. Roads. 2007. The Scripps Coupled Ocean–Atmosphere Regional (SCOAR) model, with applications in the eastern Pacific sector. *J. Clim.*, *20*, 381–402.
- Seo, H., M. Jochum, R. Murtugudde, A. J. Miller and J. O. Roads. 2008a. Precipitation from African Easterly Waves in a coupled model of the tropical Atlantic. *Journal of Climate*, *21*, 1417–1431.
- Seo, H., R. Murtugudde, M. Jochum and A. Miller. 2008b. Modeling of mesoscale coupled ocean–atmosphere interaction and its feedback to ocean in the western Arabian sea. *Ocean Model.*, *25*, 120–131.
- Seo, H., A. C. Subramanian, A. J. Miller and N. R. Cavanaugh. 2014. Coupled impacts of the diurnal cycle of sea surface temperature on the Madden-Julian Oscillation. *J. Clim.*, *27*, 8422–8443.

- Seo, H. and S.-P. Xie. 2011. Response and impact of equatorial ocean dynamics and tropical instability waves in the tropical Atlantic under global warming: A regional coupled downscaling study. *J. Geophys. Res. C Oceans*, *116*, C03026.
- Seo, H., 2017. Distinct influence of air-sea interactions mediated by mesoscale sea surface temperature and surface current in the Arabian Sea. *J. Climate*, in press, <https://doi.org/10.1175/JCLI-D-16-0834.1>
- Shchepetkin, A. and J. McWilliams. 2005. The regional oceanic modeling system (ROMS): A split-explicit, free-surface, topography-following-coordinate ocean model. *Ocean Model.*, *9*, 347–404.
- Shukla, J. and Y. Mintz. 1982. The influence of landsurface evapotranspiration on the earth's climate. *Science*, *214*, 1498–1501.
- Skamarock, W. C., J. B. Klemp, J. Dudhia, D. O. Gill, D. M. Barker, M. G. Duda and X. Huang et al. 2008. A Description of the Advanced Research WRF Version 3. Rep. 895 NCAR/TN-475+STR. Boulder, Colorado: National Center for Atmospheric Research.
- Small, R. J., J. Bacmeister, D. Bailey, A. Baker, S. Bishop, F. Bryan and J. Caron et al. 2014. A new synoptic scale resolving global climate simulation using the Community Earth System Model. *J. Adv. Model. Earth Syst.*, *6*, 1065–1094.
- Small, R. J., T. Campbell, J. Teixeira, S. Carniel, T. A. Smith, J. Dykes and S. Chen et al. 2011. Air-sea interaction in the Ligurian Sea: Assessment of a coupled ocean–atmosphere model using in situ data from LASIE07. *Mon. Weather Rev.*, *139*, 1785–1808.
- Small, R., S. de Szoeke, L. O'Neill, H. Seo, Q. Song, P. Cornillon and M. Spall et al. 2008. Air-sea interaction over ocean fronts and eddies. *Dynam. Atmos. Oceans*, *45*, 274–319.
- Small, R. J., K. J. Richards, S.-P. Xie, P. Dutrieux and T. Miyama. 2009. Damping of Tropical Instability Waves caused by the action of surface currents on stress. *J. Geophys. Res. C Oceans*, *114*, C04009.
- Somot, S., F. Sevault, M. Déqué and M. Crépon. 2008. 21st century climate change scenario for the Mediterranean using a coupled atmosphere-ocean regional climate model. *Global. Planet. Change*, *63*, 112–126.
- Stouffer, R., J. Yin, J. M. Gregory, K. W. Dixon, M. J. Spelman, W. Hurlin and A. J. Weaver et al. 2006. Investigating the causes of the response of the thermohaline circulation to past and future climate changes. *J. Clim.*, *19*, 1365–1387.
- Sutton, R. T. and D. L. R. Hodson. 2005. Atlantic Ocean forcing of North American and European summer climate. *Science*, *290*, 2133–2137.
- Taguchi, B., H. Nakamura, M. Nonaka and S.-P. Xie. 2009. Influences of the Kuroshio/Oyashio extensions on air–sea heat exchanges and storm-track activity as revealed in regional atmospheric model simulations for the 2003/04 cold season. *J. Clim.*, *22*, 6536–6560.
- Takahashi, K., A. Montecinos, K. Goubanova and B. Dewitte. 2011. ENSO regimes: Reinterpreting the canonical and Modoki El Niño. *Geophys. Res. Lett.*, *38*, L10704.
- Tang, Y. and B. Yu. 2008. MJO and its relationship to ENSO. *J. Geophys. Res.*, *113*, D14106.
- Taylor, K. E., R. J. Stouffer and G. A. Meehl. 2012. An overview of CMIP5 and the experiment design. *Bull. Am. Meteorol. Soc.*, *93*, 485–498.
- Tedeschi, R. G. and Collins, M. 2015. The influence of ENSO on South American precipitation during austral summer and autumn in observations and models. *Int. J. Climatol.*, *36*, 618–635. doi: 10.1002/joc.4371
- Teuling, A. J., M. Hirschi, A. Ohmura, M. Wild, M. Reichstein, P. Ciais and N. Buchmann et al. 2009. A regional perspective on trends in continental evaporation. *Geophys. Res. Lett.*, *36*, L02404.
- Teuling, A. J., S. I. Seneviratne, C. Williams and P. A. Troch. 2006. Observed timescales of evapotranspiration response to soil moisture. *Geophys. Res. Lett.*, *33*, L23403.

- Thornalley, D. J. R., H. Elderfield and I. N. McCave. 2010. Reconstructing North Atlantic deglacial surface hydrography and its link to the Atlantic overturning circulation, *Global. Planet. Change*, *79*, 163–175.
- Tseng, Y.-H., S. H. Chien, J. Jin and N. L. Miller. 2012. Modeling air-land-sea interactions using the Integrated Regional Model System in Monterey Bay, California. *Mon. Weather Rev.*, *140*, 1285–1306.
- Tseng, Y. H., Y. H. Lin, M. H. Lo and S. C. Yang. 2016. Diagnosing the possible dynamics controlling Sahel precipitation in the short-range ensemble Community Atmospheric Model hindcasts. *Clim. Dynam.*, *47*, 2747–2764. doi: 10.1007/s00382-016-2995-9
- Turner, A., P. Inness and J. Slingo. 2007a. The effect of doubled CO<sub>2</sub> and model basic state biases on the monsoon-ENSO system. I: Mean response and interannual variability. *Q. J. Roy. Meteorol. Soc.*, *133*, 1143–1157.
- Turner, A. G., P. M. Inness and J. M. Slingo. 2007b. The effect of doubled CO<sub>2</sub> and model basic state biases on the monsoon-ENSO system. II: Changing ENSO regimes. *Q. J. Roy. Meteorol. Soc.*, *133*, 1159–1173.
- Ulbrich, U., P. Lionello, D. Belušić, J. Jacobeit, P. Knippertz, F. G. Kuglitsch and G. C. Leckebusch et al. 2012. Climate of the Mediterranean: Synoptic patterns, temperature, precipitation, winds, and their extremes *in* *The Climate of the Mediterranean Region, from the Past to the Future*. P. Lionello, ed. Dordrecht: Elsevier, 301–346.
- USDOE (United States Department of Energy). 2015. The Model Coupling Toolkit. Last modified June 19, 2015. <http://www.mcs.anl.gov/research/projects/mct/>
- Uppala, S., P. Kallberg, A. Simmons, U. Andrae, V. Bechtold, M. Fiorino and J. Gibson et al. 2005. The ERA-40 re-analysis. *Q. J. Roy. Meteorol. Soc.*, *131*, 2961–3012.
- van den Hurk, B., M. Best, P. Dirmeyer, A. Pitman, J. Polcher and J. Santanello. 2011. Acceleration of land surface model development over a decade of glass. *Bull. Am. Meteorol. Soc.*, *92*, 1593–1600.
- Vecchi, G., B. Soden, A. Wittenberg, I. Held, A. Leetmaa and M. Harrison. 2006. Weakening of tropical Pacific atmospheric circulation due to anthropogenic forcing. *Nature*, *441*, 73–76.
- Visbeck, M., E. P. Chassignet, R. G. Curry, T. L. Delworth, R. R. Dickson and G. Krahnmann. 2003. The ocean's response to North Atlantic Oscillation variability *in* *The North Atlantic Oscillation: Climatic Significance and Environmental Impact*. J. W. Hurrell, Y. Kushnir, G. Ottersen and M. Visbeck, eds. Washington, D. C.: American Geophysical Union. doi: 10.1029/134GM06
- Visbeck, M., H. Cullen, G. Krahnmann and N. Naik. 1998. Ocean model's response to North Atlantic Oscillation-like wind forcing. *Geophys. Res. Lett.*, *25*, 4521–4524.
- Volkov, D. L. and H.M. van Aken. 2003. Annual and interannual variability of sea level in the northern North Atlantic Ocean. *J. Geophys. Res.*, *108*, 3204.
- Wang, C. and D. B. Enfield. 2001. The tropical Western Hemisphere warm pool. *Geophys. Res. Lett.*, *28*, 1635–1638.
- Wang, C. and D. B. Enfield. 2003. A further study of the tropical Western Hemisphere warm pool. *J. Clim.*, *16*, 1476–1493.
- Wang, C., D. B. Enfield, S.-K. Lee and C. W. Landsea. 2006. Influences of the Atlantic warm pool on Western Hemisphere summer rainfall and Atlantic hurricanes. *J. Clim.*, *19*, 3011–3028.
- Wang, C., S.-K. Lee and D. B. Enfield. 2008. Atlantic warm pool acting as a link between Atlantic multidecadal oscillation and Atlantic tropical cyclone activity. *Geochem. Geophys. Geosyst.*, *9*, Q05V03.
- Wang, C., C. Deser, J.-Y. Yu, P. DiNezio, and A. Clement. 2017. El Niño and Southern Oscillation (ENSO): A Review. In: *Coral Reefs of the Eastern Tropical Pacific*, Eds, P. W. Glynn, D. P. Manzello, I. C. Enochs, Springer, pp. 85–106.

- Wang, L., W. Chen and R. Huang. 2008. Interdecadal modulation of PDO on the impact of ENSO on the east Asian winter monsoon. *Geophys. Res. Lett.*, *35*, L20702.
- Warner, J. C., N. Perlin and E. Skillingstad. 2008. Using the Model Coupling Toolkit to couple earth system models. *Environ. Model. Software*, *23*, 1240–1249.
- Warner, J. C., C. R. Sherwood, R. P. Signell, C. Harris and H. G. Arango. 2008. Development of a three-dimensional, regional, coupled wave, current, and sediment-transport model. *Comput. Geosci.*, *34*, 1284–1306.
- Watanabe, M., H. Shiogama, H. Tatebe, M. Hayashi, M. Ishii and M. Kimoto. 2014. Contribution of natural decadal variability to global warming acceleration and hiatus. *Nat. Clim. Change*, *4*, 893–897.
- Weiss, M., P. Miller, B. J. J. M. van den Hurk, S. ÂˆtefÃ£nescu, R. Haarsma, L. H. van Ulft and W. Hazeleger et al. 2014. Contribution of dynamic vegetation phenology to decadal climate predictability. *J. Clim.*, *27*, 8563–8577.
- Weiss M., B. van den Hurk, R. Haarsma and W. Hazelger. 2012. Impact of vegetation variability on potential predictability and skill of EC-Earth simulations. *Clim. Dynam.*, *39*, 2733–2746.
- Wittenberg, A. T. 2009. Are historical records sufficient to constrain ENSO simulations? *Geophys. Res. Lett.*, *36*, L12702.
- Wood, R. A., A. B. Keen, J. F. B. Mitchell and J. M. Gregory. 1999. Changing spatial structure of the thermohaline circulation in response to atmospheric CO<sub>2</sub> forcing in a climate model. *Nature*, *399*, 572–575.
- Wood, R., C. R. Mechoso, C. S. Bretherton, R. A. Weller, B. Huebert, F. Straneo and B. A. Albrecht et al. 2011. The VAMOS Ocean-Cloud-Atmosphere-Land Study Regional Experiment (VOCALS-REx): Goals, platforms, and field operations. *Atmos. Chem. Phys.*, *11*, 627–654.
- Xiang, B., B. Wang, Q. Ding, F.-F. Jin, X. Fu and H.-J. Kim. 2011. Reduction of the thermocline feedback associated with mean SST bias in ENSO simulation. *Clim. Dynam.*, *39*, 1413–1430.
- Xie, S., C. Deser, G. Vecchi, J. Ma, H. Teng and A. Wittenberg. 2010. Global warming pattern formation: Sea surface temperature and rainfall. *J. Clim.*, *23*, 966–986.
- Xie, S.-P. 2004. Satellite observations of cool ocean-atmosphere interaction. *Bull. Am. Meteorol. Soc.*, *85*, 195–209.
- Xoplaki, E., J. F. Gonzalez-Rouco, J. Luterbacher and H. Wanner. 2004. Wet season Mediterranean precipitation variability: Influence of large-scale dynamics and trends. *Clim. Dynam.*, *23*, 63–78.
- Xu, H., M. Xu, S.-P. Xie and Y. Wang. 2011. Deep atmospheric response to the spring Kuroshio over the East China Sea. *J. Clim.*, *24*, 4959–4972.
- Xue, Y., F. De Sales, W. K.-M. Lau, A. Boone, J. Feng, P. Dirmeyer and Z. Guo. 2010. Intercomparison and analyses of the climatology of the West African Monsoon in the West African Monsoon Modeling and Evaluation project (WAMME) first model intercomparison experiment. *Clim. Dynam.*, *35*, 3–28.
- Yeager, S. and G. Danabasoglu. 2014. The origins of late-twentieth-century variations in the large-scale North Atlantic circulation. *J. Clim.*, *27*, 3222–3247.
- Yeh, S.-W., Y.-J. Kang, Y. Noh and A. J. Miller. 2011. The North Pacific climate transitions of the winters of 1976/77 and 1988/89. *J. Clim.*, *24*, 1170–1183.
- Yeh, S.-W., J.-S. Kug, B. Dewitte, M.-H. Kwon, B. Kirtman and F.-F. Jin. 2009. El Niño in a changing climate. *Nature*, *461*, 511–514.
- Zeng, N., J. D. Neelin, K. M. Lau and C. J. Tucker. 1999. Enhancement of interdecadal climate variability in the Sahel by vegetation interaction. *Science*, *286*, 1537–1540.
- Zhang, R. 2008. Coherent surface-subsurface fingerprint of the Atlantic meridional overturning circulation. *Geophys. Res. Lett.*, *35*, L20705.

Ziv, B., H. Saaroni and P. Alpert. 2004. The factors governing the summer regime of the Eastern Mediterranean. *Int. J. Climatol.*, 24, 1859–1871.

Received: 14 October 2015; revised: 22 August 2016.

*Editor's note:* Contributions to *The Sea: The Science of Ocean Prediction* are being published separately in special issues of *Journal of Marine Research* and will be made available in a forthcoming supplement as Volume 17 of the series.